

Neuroprotective effect of *Hibiscus sabdariffa* extract against high glucose-induced toxicity in Neuro-2a cells and *Caenorhabditis elegans*

Dicson Sheeja Malar^{a,b}, Mani Iyer Prasanth^{a,b}, James Michael Brimson^{a,b}, Kanika Verma^c, Anchalee Prasansuklab^{a,d} and Tewin Tencomnao^{a,b,*}

^aNatural Products for Neuroprotection and Anti-ageing Research Unit, Chulalongkorn University, Bangkok, Thailand

^bDepartment of Clinical Chemistry, Faculty of Allied Health Sciences, Chulalongkorn University, Bangkok, Thailand

^cICMR- National Institute of Malaria Research (NIMR), New Delhi, India

^dCollege of Public Health Sciences, Chulalongkorn University, Bangkok, Thailand

Received 3 June 2022

Accepted 18 January 2023

Pre-press 3 March 2023

Published 18 May 2023

Abstract.

BACKGROUND: Chronic hyperglycemic conditions can activate aberrant metabolic pathways causing neurotoxicity.

OBJECTIVE: This study aimed to explore the effect of ethanol extract of *Hibiscus sabdariffa* calyxes (HS) against high glucose-induced neurotoxicity in Neuro-2a cells and *Caenorhabditis elegans*.

METHODS: To ascertain the neuroprotective effect, Neuro-2a cells were pre-treated with HS followed by high glucose and assessed for cell viability, reactive oxygen species (ROS) generation, alterations in mitochondrial membrane potential ($\Delta\Psi_m$) using confocal microscopy, Real-Time PCR, Western blot and *in silico* approaches for the compounds identified through LC-MS/MS analysis. Further, *C. elegans* were treated with HS extract in the presence of glucose and analyzed for the neuroprotective effect.

RESULTS: High glucose exhibited toxicity in Neuro-2a cells by ROS generation, disrupting $\Delta\Psi_m$, modulating stress response and lipid metabolism genes, altering signaling proteins (AKT, JNK), and apoptosis (P53, Caspase-3). However, pre-treatment with HS extract reversed the effect and exhibited neuroprotection. Compounds including allo-Aromadendrene, and N-Feruloyltyramine were identified through LC-MS/MS analysis. Docking studies against candidate protein targets indicated that the compounds of HS extract exhibit higher docking scores and can inhibit/activate the targets. Further, HS extended the lifespan of *C. elegans* (CL2006) from high glucose toxicity through the downregulation of A β .

CONCLUSION: Our results propose that HS with its active constituents can be considered a promising therapeutic agent to treat hyperglycemia associated neurodegenerative diseases.

Keywords: Oxidative stress, hyperglycemia, lipid metabolism, *Seladin-1*, *C. elegans*

1. Introduction

The term neurodegenerative diseases (NDDs) symbolize a range of neurological dysfunction with diverse clinical and pathological symptoms affecting specific brain areas and halting their

*Corresponding author: Tewin Tencomnao, Chulalongkorn University, 254 Phaya Thai Rd, Wang Mai, Pathum Wan, Bangkok 10330, Thailand. Tel.: +66 2 218 1533; E-mail: tewin.t@chula.ac.th.

everyday functions [1]. With the increase in the life expectancy of people due to the advancement in medicine and given the correlation between ageing and neurodegeneration, it can be envisaged that the prevalence and incidence of neurodegenerative disorders are increasing progressively [2]. In addition to ageing, recent studies have exposed possible associations between metabolic diseases like diabetes mellitus (DM) and neurodegeneration. Being a high energy-consuming organ, the brain depends on glucose to fuel its respective functions. However, chronic hyperglycemic conditions promote oxidative stress and activate aberrant metabolic pathways causing neurotoxicity [3, 4]. Several case studies suggest that individuals with DM have a significantly increased risk of developing dementia, Alzheimer's disease (AD) and related pathologies [5–8]. The long-term hyperglycemic condition has been reported to increase amyloid beta ($A\beta$) production and accumulation in experimental animals by inducing its synaptic release, altering amyloid precursor protein (APP) processing by stimulating β -secretase, GSK-3 β or reducing the degradation through an insulin-degrading enzyme (IDE) [9–12]. Further, hyperglycemia could also exacerbate tau hyperphosphorylation and aggravate α -synuclein aggregation leading to cognitive impairment [13–15].

With the link between hyperglycemia and neurodegenerative diseases intensified, assessment of anti-diabetic drugs like insulin, metformin, and thiazolidinediones for cognitive improvement was demonstrated through pre-clinical and early clinical studies [16–21]. Further, reports from cellular and animal models of diabetic-associated neurodegeneration have exposed the role of oxidative stress and the deterioration of the antioxidant defense system during the progression of the disease. In this regard, bioactive compounds, phytochemicals, and plant extracts with antioxidant potentials are extensively focused on managing diabetic-associated neurodegenerative diseases [22–26].

Caenorhabditis elegans is a small, non-parasitic nematode with short life cycle, easy manipulation, and ~83% human homologous genes facilitate its use in age-related diseases and drug research [27]. Concerning AD, researchers have developed *C. elegans* transgenic models, which could express human $A\beta$ in the body wall muscle cells and also exhibiting paralysis phenotype. In the case of CL2006 transgenic strain, in addition to the paralysis phenotype, it also shows roller phenotype instead of normal

sinusoidal movement making it easily recognizable during maintenance and propagation [28–30].

Hibiscus sabdariffa (HS), commonly referred to as Roselle, widely cultivated throughout tropical and subtropical regions belongs to the family Malvaceae and is traditionally used as herbal medicine [31, 32]. The plant leaves are used as vegetables, and calyxes are used to prepare hot and cold beverages [33]. Pioneering studies have reported on the medicinal properties of the various parts of the plant, including anti-diabetic, anti-lipidemic, anti-hypertensive, neuroprotective, cardioprotective and anti-inflammatory. Consumption of Rosella-Stevia tea has been reported to lower blood glucose levels in individuals with diabetes [34]. Supplementation of HS and *Lippia citriodora* polyphenolic extract in grade I obese population has shown a significant decrease in appetite sensa, favouring weight reduction [35]. Consumption of roselle calyxes drink for 30 days in healthy individuals was reported to improve the health status with no serious adverse effects [36]. Polyphenolic extract of HS inhibited hyperglycemia and glycation induced-oxidative stress in the type 2 diabetic rat model [37]. Calyx extract was reported to protect neuronal cells from iron toxicity by ameliorating oxidative stress in neuronal cells [38]. Ethyl acetate fraction from HS exerted anti-hyperglycemic and neuroprotective effects in streptozotocin-induced mice by improving the cholinergic system and antioxidant mechanism [39]. Our research group has previously reported the neuroprotective effect of HS against glutamate-induced toxicity in HT-22 cells [40]. In the present study, ethanol extract of HS calyxes was assessed for its neuroprotective efficacy against high glucose-induced neuronal toxicity in Neuro-2a cells and the nematode model *Caenorhabditis elegans*.

2. Materials and methods

2.1. Chemicals

All the cell culture mediums used in the study were procured from HyClone, USA. Monoclonal rabbit primary antibodies (JNK, p-JNK, AKT, p-AKT, SIRT-1, cleaved Caspase-3, Nrf-2 and β -actin) were obtained from Cell Signaling Technology, USA. Anti-rabbit IgG- HRP linked secondary antibody, D-Glucose, Acetylcholinesterase enzyme (AChE), acetylthiocholine iodide (ATCI), and dithionitrobenzoic acid (DTNB) were purchased from Sigma

Aldrich, USA. ECL Western blotting substrate was obtained from GE Healthcare, USA. The murine neuroblastoma cells, Neuro-2a were procured from Health Science Research Resources Bank, Osaka, Japan. The chemicals required for *C. elegans* media were purchased from Himedia, India.

2.2. Plant collection and extraction

The red calyxes of *Hibiscus sabdariffa* flowers, brought from a local market in Khlong Luang District, Thailand, were separated, cleaned and dried. Plant authentication, extraction using ethanol, stock preparation and storage were done as reported earlier [40]. The working solution was prepared in MilliQ water, sterile filtered with a 0.2 µm pore size syringe filter and used for the experimental analysis.

2.3. Compound identification by LC-MS/MS analysis

The ethanol extract of HS was subjected to LC-MS/MS analysis to identify bioactive compounds. Separation was performed using a Thermo Scientific C18 column (Acclaim™ Polar Advantage II, 3 × 150 mm, 3 µm particle size) on an UltiMate 3000 UHPLC system (Dionex). Gradient elution was done at a 0.4 ml/min flow rate at 40°C column temperature using H₂O + 0.1% Formic Acid (A) and 100% Acetonitrile (B) with 22 minutes total run time. The injection volume of the sample was 3 µl. The gradient started at 5% B (0–3 min); 80% B (3–10 min); 80% B (10–15 min) and 5% B (15–22 min). High-resolution mass spectrometry was performed using a MicroTOF QIII Bruker Daltonic with ESI positive ionization. The settings were fixed as capillary voltage: 4500 V; nebulizer pressure: 2.0 bar; drying gas: 8 L/min at 250°C. The obtained peaks and the corresponding m/z values were analyzed with the METLIN database (Tolerance – 30 PPM; Charge – Positive; Adducts – M+H and M+Na), as well as the calculated theoretical masses of compounds that were previously reported in HS to identify compounds.

2.4. Cholinesterase inhibitory assay

Acetylcholinesterase inhibitory activity for ethanol extract of HS was measured according to the standard protocol [41]. To 0.1 U (10 µl) AChE, 100–500 µg/ml of HS extract was added and incubated for 45 min in a 96-well plate. The reaction

was stalled by adding 50 mM Tris-HCl, pH 8.0. Finally, 125 µl of 3 mM DTNB and 50 µl of 15 mM ATCI were added, and the absorbance was measured at 405 nm for 3 min at 1 min interval. The specific activity (U/mg of protein) of AChE was calculated using the formula given below and the percentage of inhibition was further calculated. The IC₅₀ values were further calculated using Probit software.

Specific activity (SA) =

$$\frac{\Delta A(\text{change in OD/min}) \times \text{reaction volume} \times 1000}{\epsilon \lambda \times \text{protein concentration} \times \text{sample volume}} \quad (1)$$

2.5. Cell viability assay

Neuro-2a cells (2×10^5 cells) were seeded in a 96-well plate (DMEM containing 4.5 g/L glucose, 10% Fetal bovine serum, 1X Penicillin-Streptomycin) and allowed to grow overnight. The cells were treated with various doses of glucose (50–200 mM) and HS extract (20–100 µg/ml) for 24 h and subjected to MTT assay to find the toxic dose of glucose and the non-toxic dosage range of extract. To see the protective effect of HS extract, Neuro-2a cells were pre-treated (2 h) with HS extract (1–20 µg/ml) followed by glucose treatment (175 mM) and incubated for 24 h. After incubation, cells were subjected to the MTT assay, and the absorbance was measured at 540 nm [42].

2.6. Measurement of reactive oxygen species (ROS) level

The generation of ROS upon glucose treatment was measured both qualitatively and quantitatively. Neuro-2a cells (2×10^5 cells) were grown in a 96-well black plate for quantification. Cells were pre-treated with HS extract (7.5, 10 µg/ml) for two h and then 175 mM glucose. After treatment, cells were washed with PBS and DCFH-DA (10 µM) was added and incubated for 30 min in a CO₂ incubator at 37°C. Cells were processed according to the standard protocol. The fluorescence was measured using EnSpire Multimode Plate Reader (PerkinElmer, Waltham, MA, USA) with excitation and emission of 480 and 535 nm, respectively. For qualitative analysis, Neuro-2a cells were grown on coverslips in 6-well plates, and the treatment was performed as mentioned earlier and imaged under a ZEISS LSM 700 confocal microscope [40].

2.7. Measurement of mitochondrial membrane potential ($\Delta\Psi_m$)

Cells were treated in 96-well black plates as mentioned in section 2.5. After treatment, cells were incubated with 5 μ M Rhodamine 123 (Rh 123) for 30 min, followed by washing twice with PBS and measurement of fluorescence intensity at excitation and emission of 480 and 535 nm, respectively, using EnSpire Multimode Plate Reader. For imaging, cells grown in coverslip were washed with PBS after treatment and incubated with 5 μ M Rh123 for 30 min and viewed under a ZEISS LSM 700 confocal microscope [43].

2.8. Real-Time PCR analysis

After treatment of cells, as mentioned earlier, the cells were collected, and total RNA was extracted using the standard Trizol procedure and quantified. The extracted RNA (1000 ng) was reverse-transcribed real-time PCR (qPCR) analysis was performed with Green Star PCR Master Mix (Bioneer, Korea) with gene-specific primers (Table 1), and the data were normalized to the endogenous control (GAPDH) [40].

2.9. Western blot analysis

The cells after treatment were collected and lysed with NP-40 lysis buffer. Separation of proteins (50 μ g) was done on 12% SDS gels and subsequently transferred to polyvinylidene difluoride (PVDF) membranes. Overnight blocking of the membrane was done in 5% skim milk, which is followed by 6 h incubation with respective primary antibodies (Nrf-2 (1:5000), JNK (1:2000), p-JNK (1:2000), AKT (1:2000), p-AKT (1:2000), SIRT-1 (1:5000), cleaved Caspase-3 (1:5000), p53 (1:2000), β -actin (1:5000)). Subsequently, the membranes were incubated for one h with anti-rabbit IgG-HRP linked secondary anti-body (1:10000). The bands were developed with ECL Western blot detection reagent, imaged and further quantified with ImageJ software [40].

2.10. Molecular docking analysis

The structures of the target proteins Acetylcholinesterase (4EY7), FOXO-1 (3CO7), Calpain-1 (2R9C), GSK-3 β (1R0E), LXR- α (3IPQ), and LXR-

β (1PQ6) were retrieved from PDB database. Later, the water molecules, other ligands and cofactors were removed from the protein structures, followed by energy minimization using Swiss-PDBViewer software [44]. The ligand structures were downloaded from Pubchem database. To gain insight into the possible mode of action of the active hits, the possible interactions with protein by docking simulations were studied using DockThor. This program uses a grid-based docking method to compute different modes of ligand binding on the protein. We have performed blind docking with standard mode feature of the tool [45]. Docking calculations were conducted with a grid generation of 40 \times 40 \times 40 grid size for the target protein and the results were compared with the respective positive controls for each protein.

2.11. ADMET prediction of potential phytochemicals from HS extract

Pharmacokinetic properties of drug like small molecules based on their molecular structures were predicted by SwissADME online server (<http://www.swissadme.ch>) [46]. Prediction for toxicity of the phytochemicals were performed ProTox-II webserver (https://toxnew.charite.de/protox_II/index.php?site=home) [47].

2.12. *Caenorhabditis elegans* strains and culture conditions

The wild type *C. elegans* strain N2 and the transgenic strain CL2006 expressing human A β were purchased from Caenorhabditis Genetics Centre. The strains were regularly maintained at 15°C in a nematode growth medium (NGM) agar plate using a standard protocol [48].

2.13. Lifespan assay

Lifespan analysis of *C. elegans* strains and the protective effect of HS against glucose toxicity was analyzed in liquid media as explained below. Age synchronized young adult nematodes (N2; 10 numbers/well) were seeded in a 24-well plate containing 1% FUDR and treated with glucose (100–600 mM) to optimize the toxic dose. From the previous studies, HS at concentrations of 30 and 40 μ g/ml showed an increase in lifespan in the wild type nematodes

Table 1
List of genes and sequences of primers used for Real-Time PCR analysis

Sl. No.	Gene Name	Gene ID	Forward Primer	Reverse Primer
1	<i>NQO-1</i>	18104	GTTTCTGTGGCTTCCAGGTC	CGTTTCTTCCATCCTTCCAG
2	<i>HO-1</i>	15368	TGCTCGAATGAACACTCTGG	TCCTCTGTCAGCATCACCTG
3	<i>Cyp-D</i>	67738	CTCATCTGGACGGGAAACAT	CCAGTCATCCCCCTTCTTCA
4	<i>Grp-78</i>	14828	TGCAGCAGGACATCAAGTTC	TTTCTTCTGGGGCAAATGTC
5	<i>GADD153</i>	13198	CTGCCTTTCACCTTGGAGAC	CGTTTCTGTTGGGATGAGATA
6	<i>Calpain-1</i>	12333	CTGGAGGCTGCAGGAACTAC	CTCCCGGTTGTCATAGTCGT
7	<i>GSK-3β</i>	56637	CAGTGGTGTGGATCAGTTGG	ATGTGCACAAGCTTCCAGTG
8	<i>FOXO-1</i>	56458	AACCAGTCCAACTCGACCAC	TGTCATAAAGTCGGTGCTG
9	<i>LXR-α</i>	22259	GCAGGACCAGCTCCAAGTAG	GGCTCACCAGCTTCATTAGC
10	<i>LXR-β</i>	22260	AGCTCTGCCTACATCGTGGT	GTTGTAGTGGGAAGCCGAAG
11	<i>ABCA-1</i>	11303	AGCCAGAAGGGAGTGCAGA	CATGCCATCTCGGTAAACCT
12	<i>Seladin-1</i>	74754	TGTTGCCTGAGCTTGATGAC	AGCTCGTAGGCAGTGCAAAT
13	<i>GAPDH</i>	14433	TCAACGGCACAGTCAAGG	ACTCCACGACATACTCAGC
14	$\text{A}\beta$	351	CCGACATGACTCAGGATATGAAGT	CACCATGAGTCCAATGATTGCA
15	<i>act-2</i>	WormBase ID: WBGene00000064	ATCGTCCTCGACTCTGGAGATG	TCACGTCCAGCCAAGTCAAG

[40]. To find the neuroprotective effect of HS in the CL2006 strain, the nematodes were treated with HS (10–50 $\mu\text{g/ml}$), and the extension in lifespan was analyzed. The protective dose of HS (30, 40 $\mu\text{g/ml}$) in CL2006 was analyzed for the lifespan extension effect in the nematodes upon glucose-induced toxicity. The number of animals alive after every 24 h until the last animal survived was observed under a microscope and was plotted.

2.14. Real-time PCR analysis

The CL2006 strains were grouped into five (Control, Glucose treated (500 mM), HS-30 + Glucose treated, HS-40 + Glucose treated, HS-40 treated alone) and incubated for five days. After the treatment period, the nematodes were collected for RNA extraction and Real-Time PCR analysis for $\text{A}\beta$ gene expression, as explained in section 2.8, with actin as the internal control (Table 1) [49].

2.15. Statistical analysis

All the experiments were done in triplicates and expressed as Mean \pm SD. One-way ANOVA (SPSS 17, SPSS Inc., Chicago, IL) followed by Duncan's *post hoc* test was performed to compare control vs treated and $p < 0.05$ was considered as significant.

3. Results

3.1. Phytochemical screening of HS extract by LC-MS analysis

To identify the potential bioactive compounds in HS extract, LC-MS analysis have been performed. The list of possible compounds after analyzing the m/z peaks were listed in Table 2. The compounds were analyzed using the METLIN database and compared with previous literature regarding the phytochemical screening performed in *Hibiscus sabdariffa*. Compounds including Hibiscus acid, allo-Aromadendrene, N-Feruloyltyramine, Sinapoyl aldehyde, Isobetanin, Hibiscus acid hydroxyethyl ester, Anisocoumarin H, Ethyl chlorogenate, which have been already reported to be present in *Hibiscus sabdariffa* extracts have been identified.

3.2. HS extract inhibited cholinesterase enzyme *in vitro*

Cholinesterase enzyme (ChE) is a potential therapeutic target in treating Alzheimer's disease. The inhibitors of ChEs abrogate the enzymatic degradation of acetylcholine in the synaptic cleft and improve cognition and memory in AD individuals. As HS was evaluated for its neuroprotective efficacy, the impact of the extract against the acetylcholinesterase enzyme was assessed. HS extract showed significant dose-dependent inhibition of the enzyme at an IC_{50} value

Table 2
List of compounds in HS extract identified by LC-MS/MS analysis

S.No	Compound Name	Retention time (min)	m/z	Formula	Molecular Weight (g/mol)
1	2-Aminoheptanoic acid	1.5	146.1181	C ₇ H ₁₅ NO ₂	145.2
2	Hibiscus acid	2.1	190.1077	C ₆ H ₆ O ₇	190.11
3	Quinate	2.3	193.07	C ₇ H ₁₂ O ₆	192.17
4	Furfural diethyl acetal	2.5	196.0973	C ₉ H ₁₄ O ₃	170.21
5	Pyroglutamic acid	3	130.0499	C ₅ H ₇ NO ₃	129.11
6	3',4',7-Trihydroxyisoflavan	3	259.0927	C ₁₅ H ₁₄ O ₄	258.269
7	11-Hydroxycanthin-6-one	4.3	259.0418	C ₁₄ H ₈ N ₂ O ₂	236.22
8	Epigallocatechin 3-O-(3-O-methylgallate)	4.3	495.0936	C ₂₃ H ₂₀ O ₁₁	472.4
9	Hibiscus acid hydroxyethylester	4.6	237.0595	C ₈ H ₁₃ O ₈	237.18
10	5,6,7-Trimethoxycoumarin	4.6	259.0518	C ₁₂ H ₁₂ O ₅	236.22
11	3-dehydroquininate	5.5	191.0197	C ₇ H ₁₀ O ₆	190.15
12	Hydroxycitric acid	5.5	209.0292	C ₆ H ₈ O ₈	208.12
13	5-Deoxyleucopelargonidin	6.3	275.0754	C ₁₅ H ₁₄ O ₅	274.27
14	Anisocoumarin H	7	315.1544	C ₁₉ H ₂₂ O ₄	314.4
15	3'-hydroxy-n-methyl-(s)-coclaurine	7.4	316.1532	C ₁₈ H ₂₁ NO ₄	315.4
16	Pelargonidin 3-O-glucoside	7.6	456.0685	C ₂₁ H ₂₁ O ₁₀ ⁺	433.4
17	Isobetanin	8	551.158	C ₂₄ H ₂₆ N ₂ O ₁₃	550.5
18	7,8-Dihydroxycoumarin	8.2	201.0393	C ₉ H ₆ O ₄	178.14
19	3-Hydroxy-4-butanolide	8.6	265.0915	C ₁₀ H ₁₆ O ₈	264.23
20	allo-Aromadendrene	8.8	227.1765	C ₁₅ H ₂₄	204.35
21	Ethyl chlorogenate	9	383.1342	C ₁₈ H ₂₂ O ₉	382.4
22	Pelargonidin 3-rhamnoside 5-glucoside	9	580.1782	C ₂₇ H ₃₁ O ₁₄ ⁺	579.5
23	2-(2,4,7-trihydroxy-8-methoxy-1,4-benzoxazin-3-one)-b-D-glucopyranose	10.1	390.1390	C ₁₅ H ₁₉ NO ₁₁	389.31
24	Glucovanillin	10.1	315.1046	C ₁₄ H ₁₈ O ₈	314.29
25	N-Feruloyltyramine	10.1	314.1382	C ₁₈ H ₁₉ NO ₄	313.3
26	Sinapoyl aldehyde	10.8	209.0807	C ₁₁ H ₁₂ O ₄	208.21

of $92.72 \pm 2.95 \mu\text{g/ml}$ compared to the control. The standard drug donepezil exhibited higher efficiency at an IC_{50} value of $10.40 \pm 0.01 \mu\text{g/ml}$ (Fig. 1A). The results implicate the inhibitory potential of HS extract against ChE, suggesting its neuroprotective effect.

Further, the bioactive compounds identified in the HS extract were subjected to molecular docking analysis against acetylcholinesterase enzyme (AChE) with donepezil as the positive ligand. Donepezil showed a binding score of -8.32 kcal/mol . In contrast, the phytochemicals of HS, including N-Feruloyltyramine (-9.894 kcal/mol), 11-Hydroxycanthin-6-one (-9.194 kcal/mol), allo-Aromadendrene (-9.058 kcal/mol), showed higher binding score than the control indicating they

have better inhibitory property against AChE. The mode of interaction of the top 3 hits and control against the target were represented in Fig. 1B–E.

3.3. Glucose treatment exhibited dose-dependent toxicity in Neuro-2a cells, and HS extract pre-treatment showed a protective effect

Neuro-2a cells were treated with varying doses of glucose (50–200 mM) and subjected to the MTT assay to check the toxic effect of high glucose. Glucose exhibited dose-dependent cytotoxicity in Neuro-2a cells. After 24 h treatment, a significant ($p < 0.05$) reduction in the viability of cells was seen from the addition of 150 mM glucose onwards,

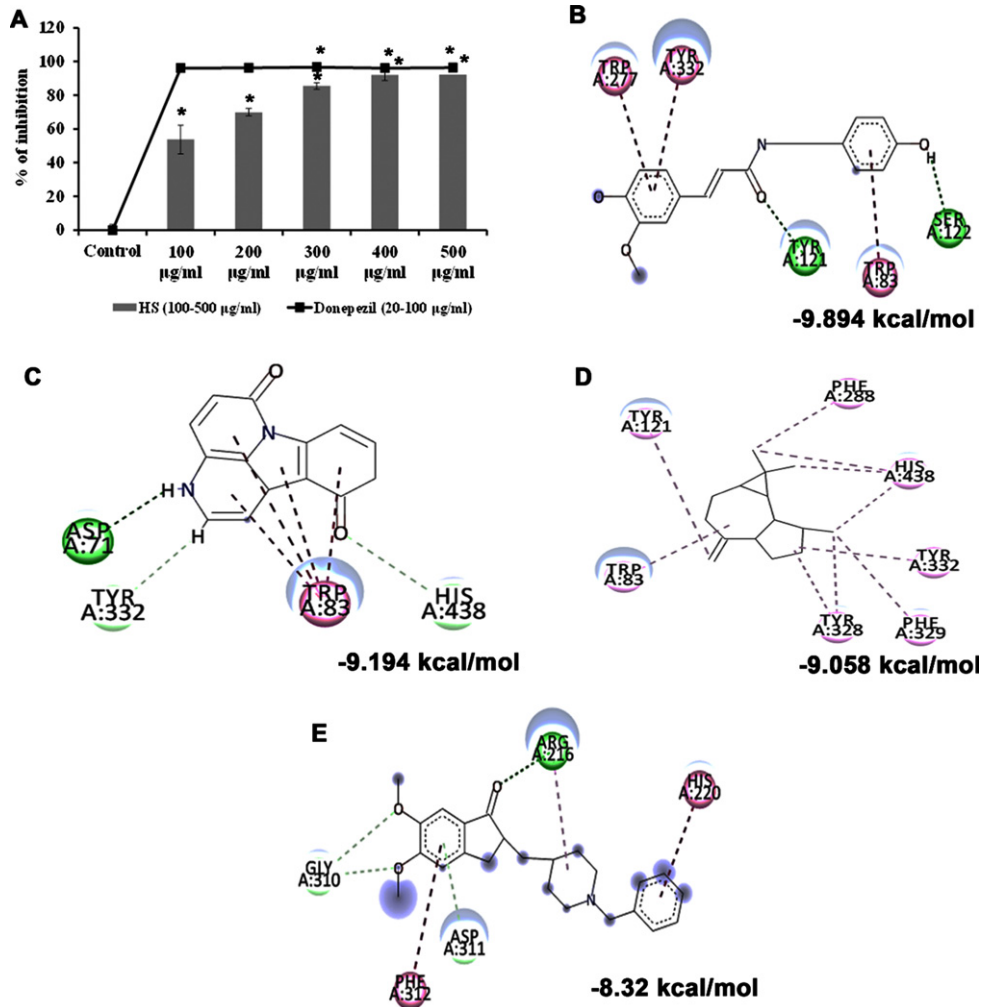


Fig. 1. (A) Acetylcholinesterase inhibitory effect of HS extract (100–500 µg/ml) and the standard drug donepezil (20–100 µg/ml). (* Control vs Donepezil/HS extract treatment; Significance at $p < 0.05$; $n = 3$). Molecular docking and interaction of compounds (top 3 hits) from HS extract against AChE (B) N-Feruloyltyramine (C) 11-Hydroxycanthin-6-one (D) allo-Aromadendrene (E) Donepezil (Green indicates hydrogen bond, purple represents alkyl bond, pink represents π -alkyl bond).

and 175 mM concentration showed a 50% reduction in viability (Fig. 2A). From the obtained results, 175 mM was fixed as the toxic dose. Further, the non-toxic dosage range of HS (20–100 µg/ml) was analyzed. No significant reduction in viability was observed until 60 µg/ml of extract (Fig. 2B). Hence, to check the protective effect of HS against high glucose-induced toxicity, the concentrations ranging from 1–20 µg/ml were analyzed. Pre-treatment of HS extract at 7.5 and 10 µg/ml showed a significant increase in viability of 86.5 ± 0.9 and $89.03 \pm 0.9\%$, respectively, against high glucose (Fig. 2C). The morphological changes in the cell upon high glucose-induced toxicity and the protective effect of HS are represented in Fig. 3. Cell shrinkage and retraction

of neurites were observed upon glucose treatment whereas, HS treatment reversed the changes in Neuro-2a cells. Based on the observed results, the 7.5 and 10 µg/ml HS concentrations were used for further experimental analysis.

3.4. Pre-treatment with HS abolishes high glucose-induced oxidative stress by inhibiting ROS formation

Previous reports suggest that high glucose-induced ROS generation is one of the critical events in making the biomolecules susceptible to harmful events and contributing to toxicity. Accordingly, exposure to high glucose significantly increased ROS genera-

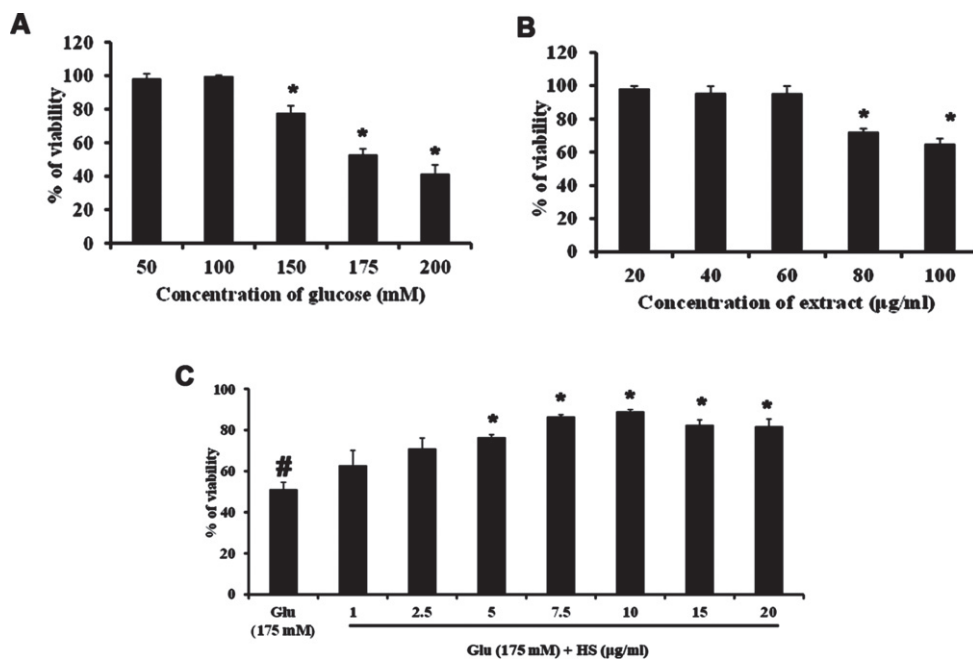


Fig. 2. Cell viability determination by MTT assay. (A) Effect of varying concentrations of glucose in Neuro-2a cells (B) Effect of HS extract in Neuro-2a cells (C) Protective effect of HS extract against high glucose (175 mM) (Significance at $p < 0.05$; # Control vs Glucose; * Glucose vs HS pre-treated; $n = 3$).

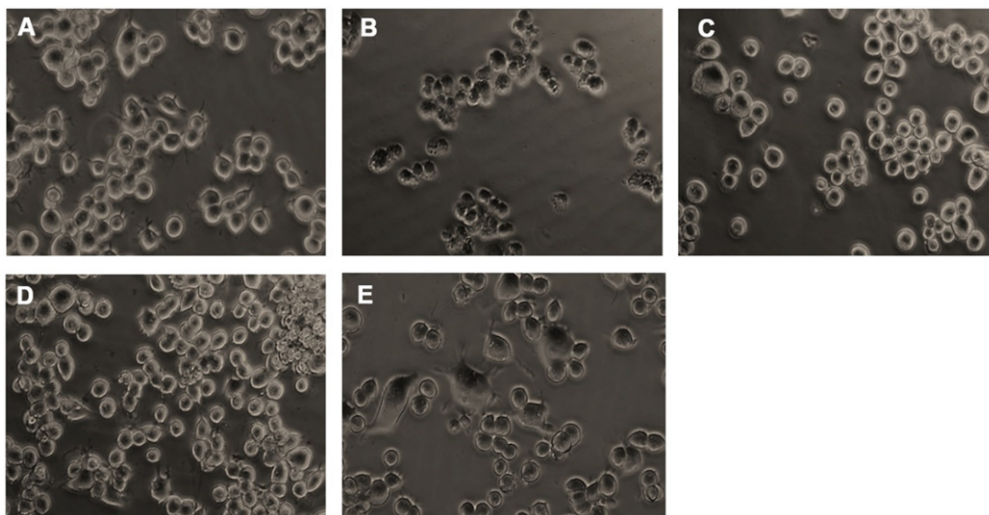


Fig. 3. Microscopic images representing restoration from glucose-induced toxicity by HS. (A) Control (B) High glucose (175 mM) (C) HS-7.5 (pre-treatment 2 h) + high glucose (D) HS-10 (pre-treatment 2 h) + high glucose (E) HS-10

tion ($159.9 \pm 1.5\%$) compared to the control, which can also be observed from the increase in fluorescence intensity in confocal microscopic images (Fig. 4B, F). Nevertheless, pre-treatment (2 h) with HS (10 µg/ml) significantly reduced ROS generation ($95 \pm 11.8\%$) compared to glucose treated group indicating the antioxidant potential (Fig. 4C–F).

3.5. HS extract restored the expression of stress response elements against high glucose-induced toxicity

With the signifying role of ROS formation in high glucose-mediated toxicity observed, the role of antioxidant response element signaling pathway

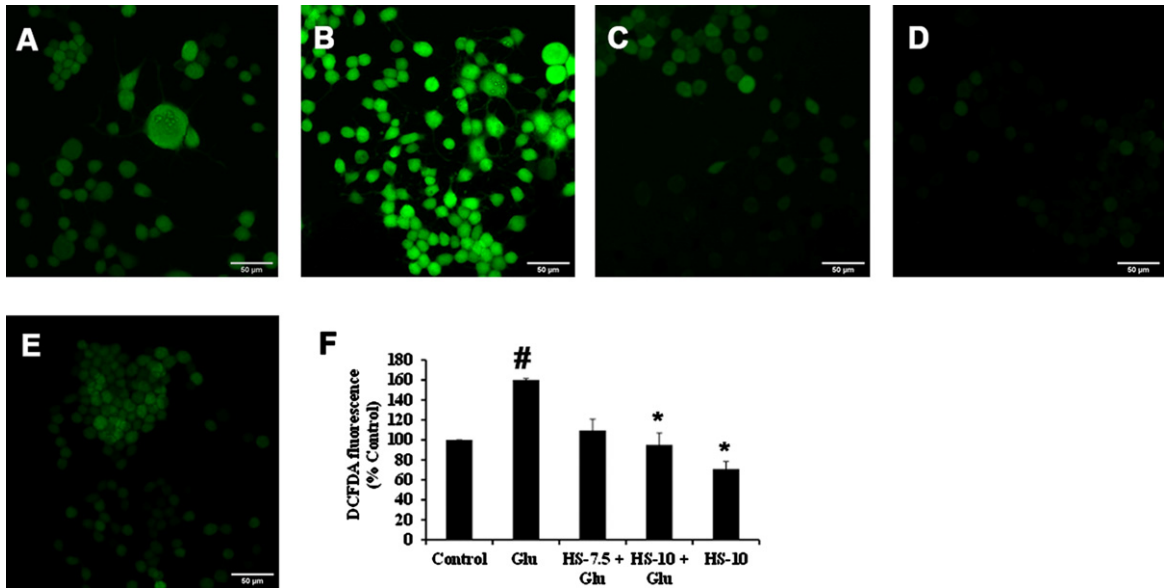


Fig. 4. Confocal microscopic images representing attenuation of ROS formation by HS. (A) Control (B) high glucose (175 mM) (C) HS-7.5 (pre-treatment 2 h) + high glucose (D) HS-10 (pre-treatment 2 h) + high glucose (E) HS-10 (F) Quantification of ROS (Significance at $p < 0.05$; # Control vs Glucose; * Glucose vs HS pre-treated; $n = 3$)

upon toxicity and the effect of HS to counterattack the response were studied using western blot (Nrf-2) and gene (NQO-1, HO-1) expression analysis. Protein expression analysis showed that upon high glucose treatment, Nrf-2 (0.89 ± 0.08 fold) levels were reduced compared to the control. At the same time, a reversal in the effect was observed upon pre-treatment with HS extract. Moreover, HS alone ($10 \mu\text{g/ml}$) significantly ($p < 0.05$) augmented the expression indicating the antioxidant potential of the extract (Fig. 5A, B). The gene expression analysis of NQO-1 and HO-1 showed a reversal in trend. High glucose treatment significantly induced the expression of NQO-1 (3.5 ± 0.2 fold) and HO-1 (1.5 ± 0.15 fold) compared to the control, whereas pre-treatment with HS ($10 \mu\text{g/ml}$) significantly ($p < 0.05$) reduced the expression of both genes compared to high glucose treatment indicating the restoration of the stress response (Fig. 5C).

3.6. HS extract restored high glucose-induced perturbations in mitochondrial membrane potential ($\Delta\Psi_m$) by diminishing Cyclophilin-D (Cyp-D) gene expression

In response to ROS generation, changes in $\Delta\Psi_m$ associated with pore formation with an increase in Cyp-D expression can be observed under oxidative stress conditions. In this regard, the perturba-

tions in $\Delta\Psi_m$ upon high-glucose induced toxicity were analyzed using Rho123 dye. Both qualitative and quantitative analysis showed that high glucose treatment reduced the $\Delta\Psi_m$, as noticed by the decrease in fluorescence intensity compared to control (Fig. 6A, B, F). Further, the gene expression of Cyp-D (1.68 ± 0.04 fold) was significantly increased ($p < 0.05$) (Fig. 6G), contributing to the mitochondrial permeability transition pore (mPTP). Meanwhile, HS pre-treatment significantly restored the $\Delta\Psi_m$ by impeding mPTP formation by inhibiting Cyp-D gene (HS-10 $\mu\text{g/ml}$; 0.77 ± 0.1 fold) (Fig. 6C–G).

3.7. HS extract regulates SIRT-1/AKT/FOXO-1 pathway and inhibits the JNK pathway against high glucose-induced toxicity

The effect of HS extract on various pathways and targets involved in hyperglycemia-induced cell death was studied by gene and protein expression analysis. Evidence suggests that endoplasmic reticulum stress (ER stress) occurs concomitantly with oxidative stress conditions under chronic hyperglycemia. The gene expression analysis shows significant upregulation of Grp78 (1.53 ± 0.09), Gadd153/CHOP (1.40 ± 0.14), Calpain-1 (2.82 ± 0.14) and GSK-3 β (1.42 ± 0.12) genes indicating ER stress and activation of downstream mechanism to trigger apoptosis (Fig. 7A). In addition, the interactions between SIRT-

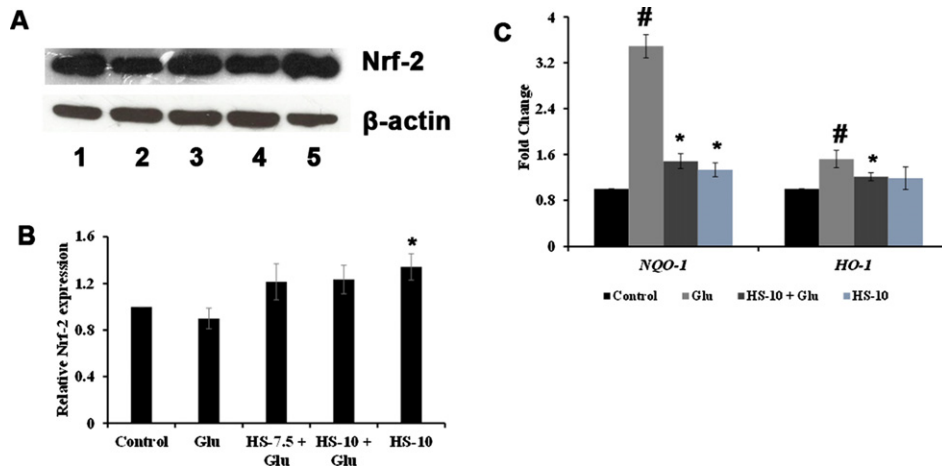


Fig. 5. Effect of HS on stress response elements against glucose induced toxicity (A) Western blot expression of Nrf-2 (Lane: 1- Control; 2- High glucose; 3- HS-7.5 (pre-treatment 2 h) + high glucose; 4- HS-10 (pre-treatment 2 h) + high glucose; 5- HS-10) (B) Quantification of Nrf-2 expression (C) Transcriptional regulation of stress response genes (*NQO-1* and *HO-1*) (Significance at $p < 0.05$; # Control vs High Glucose; * High Glucose vs HS pre-treated; $n = 3$)

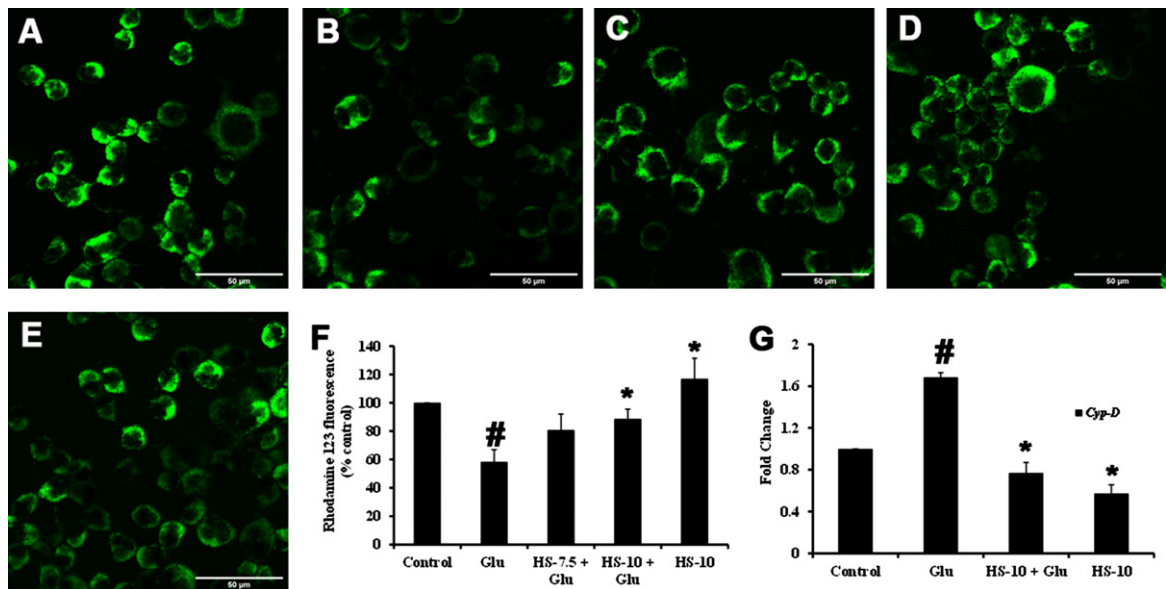


Fig. 6. Effect of HS on mitochondrial membrane potential. Confocal microscopic images representing alterations in $\Delta\Psi_m$ (A) Control (B) High glucose (175 mM) (C) HS-7.5 (pre-treatment 2 h) + high glucose (D) HS-10 (pre-treatment 2 h) + high glucose (E) HS-10 (F) Quantification of relative fluorescence of Rh123 (% control) (G) Regulation of *Cyp-D* gene expression (Significance at $p < 0.05$; # Control vs High Glucose; * High Glucose vs HS pre-treated; $n = 3$)

1 and FOXO-1 play a vital role in high glucose associated cellular stress. The results show that upon high glucose treatment, the protein expression of SIRT-1 (0.84 ± 0.07 fold) was decreased with a significant increase in the gene expression of FOXO-1 (1.28 ± 0.05 fold) (Fig. 7A–C). Also, a significant ($p < 0.05$) decrease in the ratio of p-AKT/AKT (0.69 ± 0.03 fold) and increase in p-

JNK/JNK (1.60 ± 0.17 fold) protein expression were observed, indicating alterations in the cellular signaling pathways (Fig. 7B, D). Nevertheless, HS extract pre-treatment significantly restored the changes by downregulating ER stress-associated genes, modulating the SIRT-1/AKT/FOXO-1 pathway and inhibiting the JNK pathway to protect cells from neurodegeneration (Fig. 7).

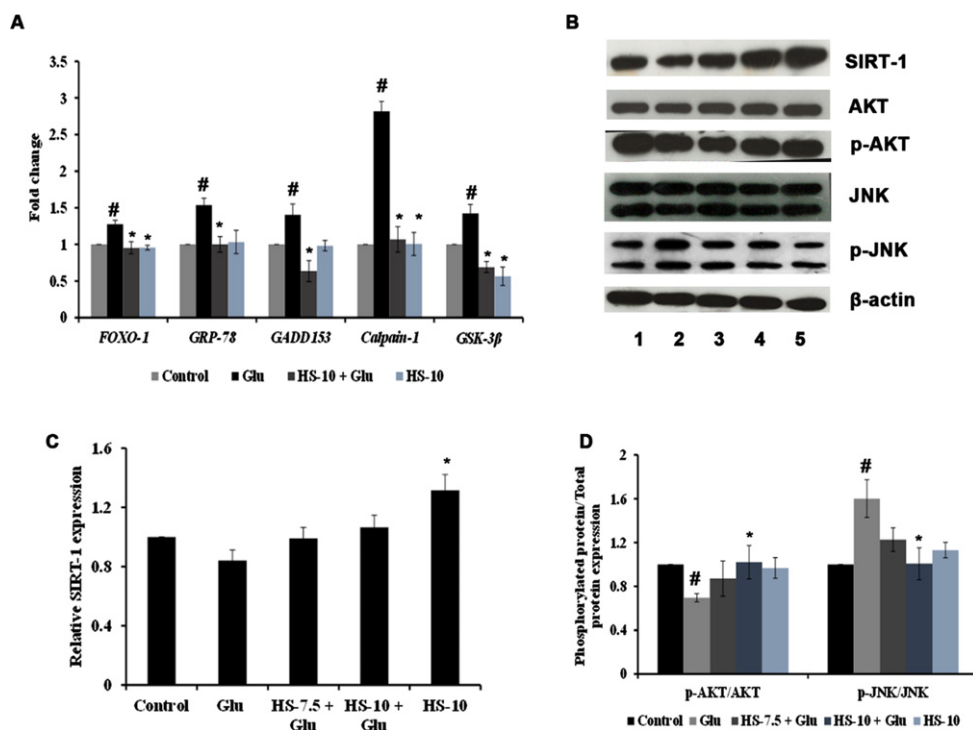


Fig. 7. (A) Transcriptional regulation of genes involved in stress response by HS extract. (B) Representative blots showing the regulation of protein expression involved in cell signaling by HS extract (Lane: 1- Control; 2- High glucose; 3- HS-7.5 (pre-treatment 2 h) + high glucose; 4- HS-10 (pre-treatment 2 h) + high glucose; 5- HS-10) (C) Quantification of relative expression of SIRT-1 (D) Ratio of phosphorylated protein to total protein expression (p-AKT/AKT and P-JNK/JNK) (Significance at $p < 0.05$; # Control vs high glucose; * high glucose vs HS pre-treated; $n = 3$).

In addition to *in vitro* studies, molecular docking studies with the bioactive compounds of HS were also carried out against the protein targets FOXO-1, Calpain-1 and GSK-3 β and the results were compared with the respective antagonists AS1842856, SNJ-1945 and LY2090314 respectively. In the case of FOXO-1, Anisocoumarin H (–8.187 kcal/mol), Pelargonidin 3-rhamnoside 5-glucoside (–8.019 kcal/mol), allo-Aromadendrene (–7.529 kcal/mol) showed higher binding efficiency when compared to the standard antagonist AS1842856 (–7.143 kcal/mol) (Fig. 8). For calpain-1, allo-Aromadendrene (–7.77 kcal/mol), Pelargonidin 3-rhamnoside 5-glucoside (–7.743 kcal/mol), Anisocoumarin H (–7.692 kcal/mol), Quercetin 3-O-(6-O-malonyl-beta-D-glucoside) (–7.66 kcal/mol), N-Feruloyltyramine (–7.539 kcal/mol) and 11-Hydroxycanthin-6-one (–7.469 kcal/mol) showed higher inhibitory potential based on their energy when compared to the standard antagonist SNJ-1945 (–7.14 kcal/mol) (Fig. 9). The compounds allo-Aromadendrene (–8.963 kcal/mol), Anisocoumarin H (–8.808 kcal/mol), 11-

Hydroxycanthin-6-one (–8.627 kcal/mol), Sinapoyl aldehyde (–8.337 kcal/mol), N-Feruloyltyramine (–7.718 kcal/mol) showed higher binding efficiency to inhibit the protein compared to the standard inhibitor LY2090314 (–7.532 kcal/mol) (Fig. 10). The ligands showed different types of interactions, including conventional hydrogen bond, alkyl bond, π -alkyl bond, carbon-hydrogen bond, and π - π bond on the binding site of the respective proteins. The interactions between the top 3 hits of the compound along with the standard against the respective targets were represented in Figs. 8–10.

3.8. HS extract upregulates glucose metabolism associated genes through the activation of LXRs against high glucose-induced neurodegeneration

High glucose-induced JNK activation causes abnormality in glucose metabolism and lipid accumulation leading to perturbations in lipid raft and the transcriptional regulation of candidate genes (LXR- α , LXR- β , Seladin-1, and ABCA-1) involved

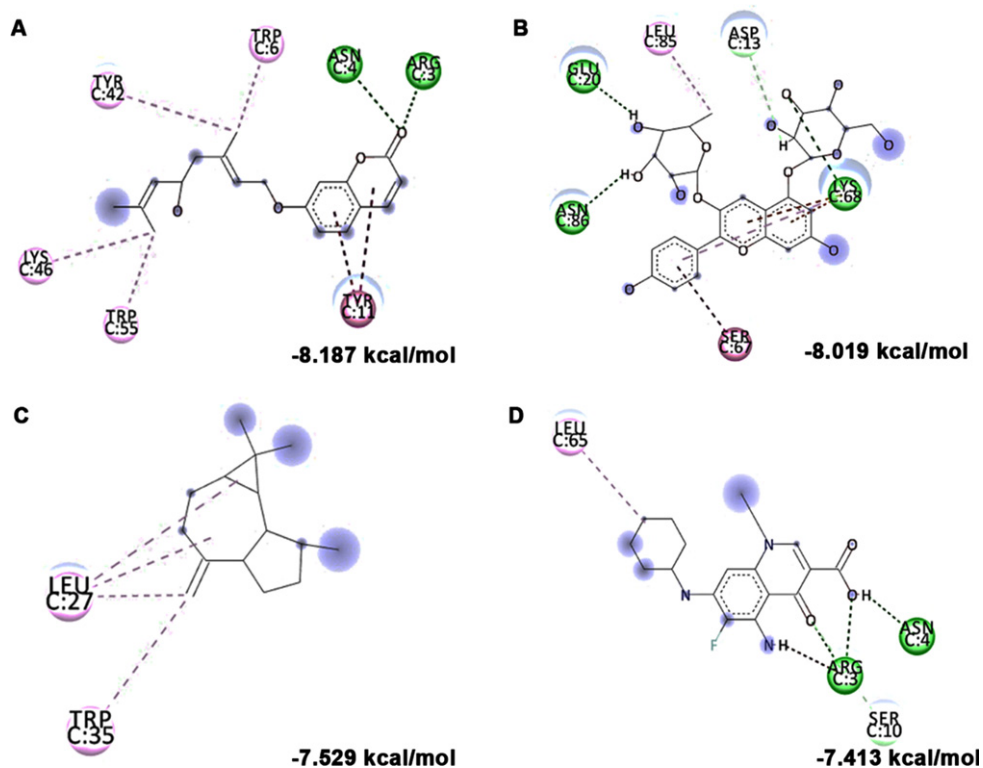


Fig. 8. Molecular docking and mode of interaction of compounds (top 3 hits) from HS extract against FOXO-1 (A) Anisocoumarin H (B) Pelargonidin 3-rhamnoside 5-glucoside (C) allo-Aromadendrene (D) AS1842856 (Green indicates hydrogen bond, purple represents alkyl bond, pink represents π -alkyl bond)

in maintaining homeostasis has been studied. Treatment with high glucose significantly downregulated both LXR- α and β (0.8 ± 0.05 and 0.53 ± 0.06 fold) and their downstream targets Seladin-1 (0.58 ± 0.04) and ABCA-1 (0.66 ± 0.06). However, a significant ($p < 0.05$) reversal in effect (LXR- α -1.72 ± 0.19 fold; LXR- β -1.16 ± 0.04 fold; Seladin-1 -1.34 ± 0.16 fold; ABCA-1 -1.07 ± 0.06 fold) has been observed upon pre-treatment with HS extract ($10 \mu\text{g/ml}$) indicating the effect of the extract to improve glucose metabolism and regulate lipid metabolism against high glucose-induced toxicity (Fig. 11). Further, molecular docking was performed against LXRs. The binding score and interactions were compared with that of the agonist GW3965 to identify the compounds of HS that could activate the pathway. Results show that the compounds including allo-Aromadendrene (-9.242 kcal/mol), 11-Hydroxycanthin-6-one (-8.969 kcal/mol), Sinapoyl aldehyde (-8.953 kcal/mol), Furfural diethyl acetal (-8.327 kcal/mol) N-Feruloyltyramine (-7.928 kcal/mol) showed higher binding score

compared to GW3965 (-7.69 kcal/mol) against LXR- α . The interactions of the top 3 hits against LXR- α are represented in Fig. 12. In the case of LXR- β , allo-Aromadendrene (-9.164 kcal/mol) and 11-Hydroxycanthin-6-one (-8.928 kcal/mol) showed higher binding scores than GW3965 (Fig. 13).

3.9. HS extract inhibits high glucose-induced apoptosis

The effect of HS extract on high glucose-induced cell death was analyzed by protein expression studies (cleaved Caspase-3, P53). The Neuro-2a cells on treatment with high glucose showed a significant ($p < 0.05$) increase in expression of cleaved Caspase-3 (1.46 ± 0.06 fold) and P53 (1.47 ± 0.29) proteins indicating activation of the apoptotic pathway. However, pre-treatment with HS extract ($10 \mu\text{g/ml}$) showed a significant reduction of both the proteins suggesting neuroprotection against high glucose-induced toxicity (Fig. 14).

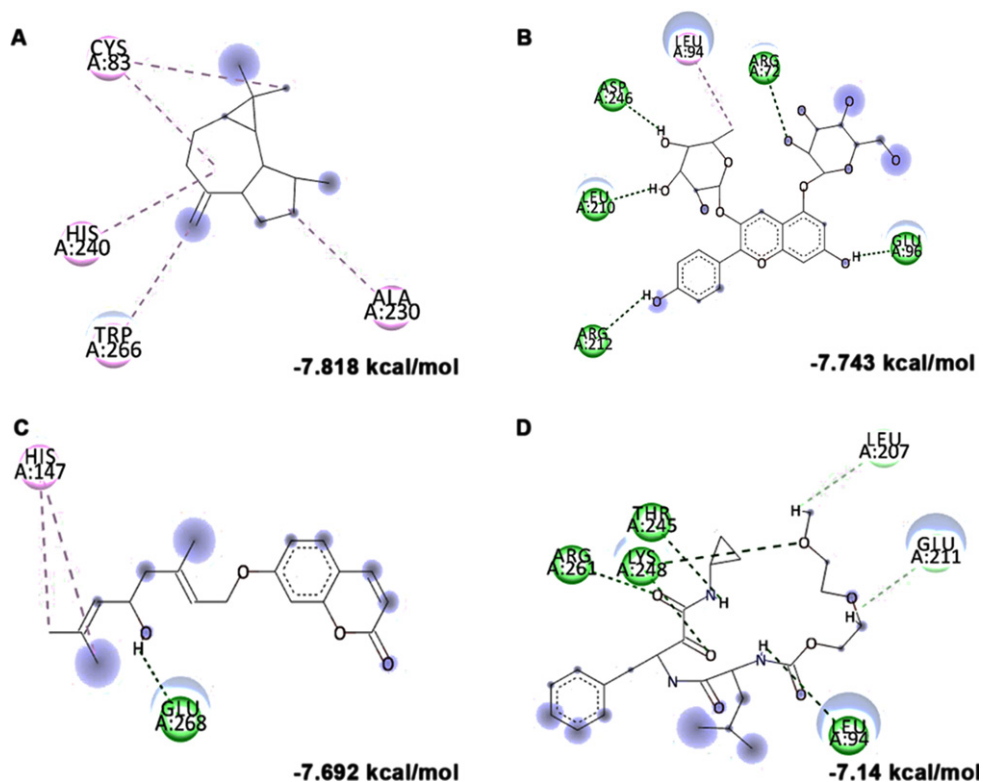


Fig. 9. Molecular docking and mode of interaction of compounds (top 3 hits) from HS extract against Calpain-1 (A) allo-Aromadendrene (B) Pelargonidin 3-rhamnoside 5-glucoside (C) N-Feruloyltyramine (D) SNJ-1945 (Green indicates hydrogen bond, purple represents alkyl bond, pink represent a π -alkyl bond, yellow represent π -sulfur interactions)

3.10. Drug-like properties of phytochemicals from HS extract

Poor absorption, distribution, metabolism and excretion (ADME) properties of a molecule have a severe impact on the drug discovery pipeline. Therefore, it is important for a small molecule to meet the ADME requirements in order to be a successful drug. Among the 26 compounds identified from HS extract, 6 compounds, which showed activity through in silico studies were taken for ADMET predictions. A molecule's bioavailability is determined by how it is absorbed and how it is processed by the liver. Based on Lipinski's rule of five (RO5), the results were analyzed for each phytochemical (Table 3). Out of 6 compounds, Epigallocatechin 3-O-(3-O-methyl)gallate showed 'n' violation value of 2, while all the other compounds fit within the acceptable limits. Further, toxicity predictions (Table 4) indicate that all the analyzed compounds are inactive to carcinogenicity, hepatotoxicity, and cytotoxicity while Epigallocatechin 3-O-(3-O-methyl)gallate and

N-feruloyltyramine showed immunotoxicity and 11-Hydroxycanthin-6-one showed mutagenicity.

3.11. HS extract revokes high glucose-mediated shortened lifespan in transgenic *C. elegans* strain CL2006 by downregulating the expression of $A\beta$

Hyperglycemia associated changes and the protective effect of HS extract were studied in the model system *C. elegans* (both wild type (N2) and transgenic strain expressing $A\beta$ (CL2006)). In the current study, the HS extract dosage of 30, 40 $\mu\text{g/ml}$ was used based on our earlier report on the effect of extending the lifespan of wild type nematodes [40]. To find the toxic dosage of glucose, N2 worms were treated with various glucose concentrations (100–600 mM). In a dose-dependent manner, glucose exhibited toxicity to the nematodes and reduced their lifespan. At the concentration of 500 mM, glucose significantly reduced the lifespan in N2 worms with average maximum survival days of 16 ± 0.70 (Fig. 15A, B), and

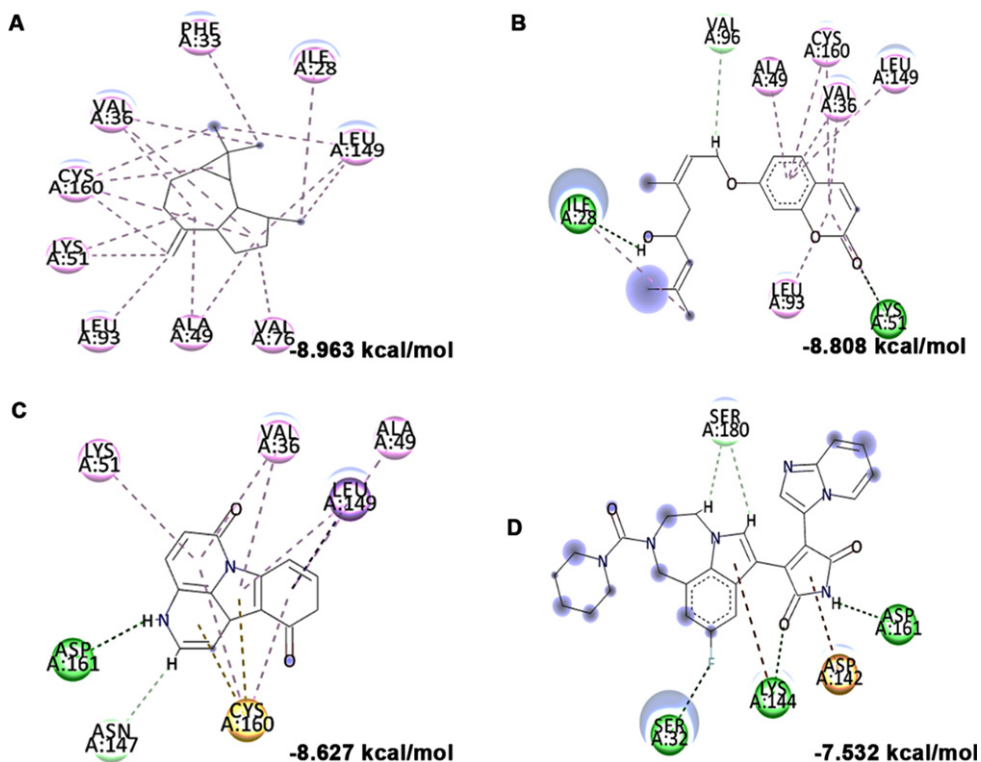


Fig. 10. Molecular docking and mode of interaction of compounds (top 3 hits) from HS extract against GSK-3 β (A) allo-Aromadendrene (B) Anisocoumarin H (C) 11-Hydroxycanthin-6-one (D) LY2090314 (Green indicates hydrogen bond, purple represents alkyl bond, pink represent a π -alkyl bond, yellow represent π -sulfur interactions)

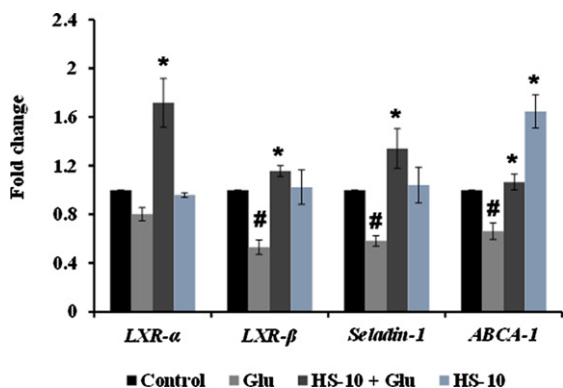


Fig. 11. Transcriptional regulation of glucose and lipid metabolism associated genes (*LXR-α*, *LXR-β*, *Seladin-1*, and *ABCA-1*) by HS extract (Significance at $p < 0.05$; # Control vs High glucose; * High glucose vs HS pre-treated; $n = 3$).

HS treatment significantly extended the lifespan of nematodes to 19.8 ± 0.44 , 21.2 ± 1.48 days for 30, 40 $\mu\text{g/ml}$ extract respectively (Fig. 15C, D).

To check the neuroprotective efficacy CL2006 strain was used and HS extract (30, 40 $\mu\text{g/ml}$)

showed significant ($p < 0.05$) extension in lifespan (20 ± 0.70 , 19.6 ± 0.55 days) when compared to control worms, which survived only for 16.6 ± 0.55 days. 13.4 ± 0.55 compared to control (21.6 ± 0.55 in N2 and 16.4 ± 0.54) (Fig. 16A, B). Likewise, HS extract (30, 40 $\mu\text{g/ml}$) extended the average maximum survival days of the CL2006 transgenic strain (17.2 ± 0.84 , 18 ± 0.71 days) significantly ($p < 0.05$) when compared to glucose treated group (12.8 ± 0.84) (Fig. 16C, D). In addition, to analyze whether high glucose-mediated shortening of lifespan is associated with increased expression of A β peptide in the Alzheimer's disease model (CL2006) gene expression. The results show that upon high glucose exposure in nematodes, a significant ($p < 0.05$) increase in A β expression was observed when compared to the control CL2006 (without glucose exposure). However, HS extract treatment significantly reduced the expression of A β in a dose-dependent manner indicating the extended lifespan in CL2006 transgenic strain by the extract could be due to the suppression of A β proteotoxicity induced by high glucose.

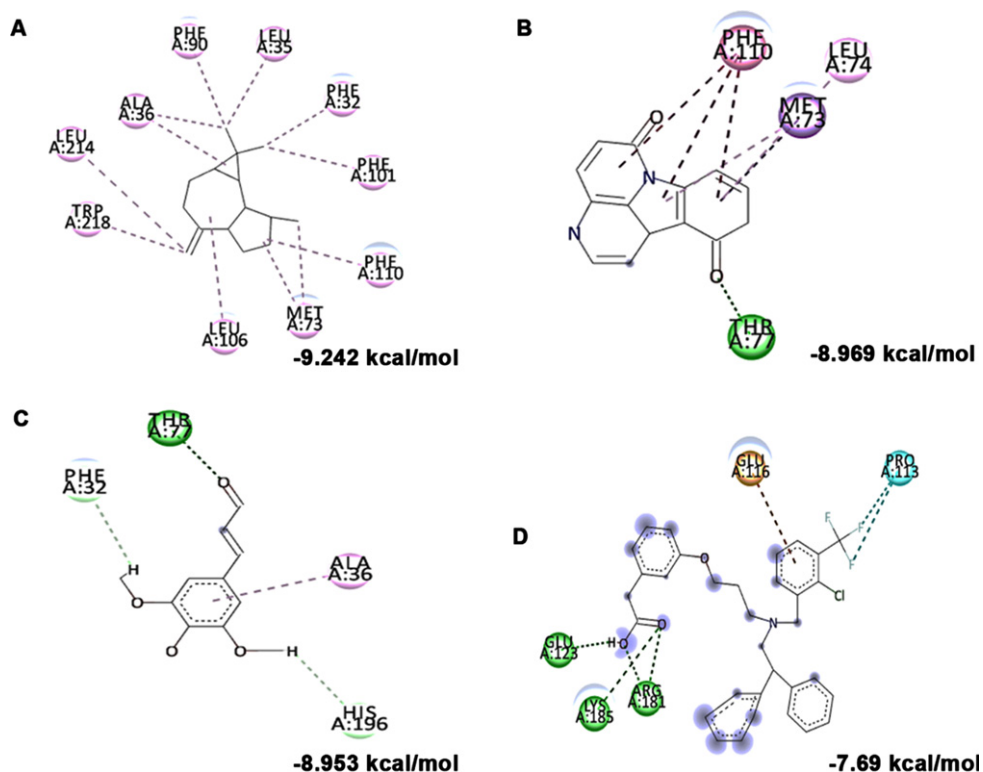


Fig. 12. Molecular docking and mode of interaction of compounds (top 3 hits) from HS extract against LXR- α (A) allo-Aromadendrene (B) 11-Hydroxycanthin-6-one (C) Sinapoyl aldehyde (D) GW3965 (Green indicates hydrogen bond, purple represents alkyl bond, pink represent π -alkyl bond)

4. Discussion

Diabetes mellitus has been constantly reported to activate or suppress several cellular pathways in the brain and is associated with cognitive dysfunction and neurodegeneration [50]. The current study is aimed to investigate the efficacy of ethanolic extract of *H. sabdariffa* calyces, a plant with both reported anti-diabetic and neuroprotective potential against high glucose-induced neurotoxicity. Hyperglycemia-induced memory impairment has been associated with a decline in cholinergic functions and increases acetylcholinesterase enzyme (AChE) activity, cleaving the neurotransmitter acetylcholine and inhibiting neurotransmission [51]. Our study shows that HS extract could significantly inhibit the cholinesterase enzyme dose-dependent, indicating the neuroprotective potential.

Pioneering studies have reported high glucose-mediated neurotoxicity in several neuronal cells [52]. Concomitantly, glucose exhibited neurotoxicity in Neuro-2a cells in a dose-dependent manner, with 175 mM showing a 50% reduction in viability at

24 h. The incidence of cell death was associated with increased ROS generation, induction of oxidative stress and inhibition of Nrf-2 expression. The results align with the previous reports stating that high glucose can evoke oxidative stress while causing alterations in the stress response mechanisms [53]. The Nrf-2 is one of the critical regulators maintaining redox homeostasis and is involved in the ROS clearance mechanisms by activating several genes involved in antioxidant defense mechanisms [54, 55]. Although it is expected to suppress downstream effectors (NQO-1 and HO-1) of Nrf-2, gene expression studies showed that upon high glucose treatment, a significant increase in the expression of both the genes. Previous studies have reported on the increase in expression of HO-1 upon high glucose treatment in diabetic mice retina and astrocytes through NADPH oxidase (Nox)/ NF- κ B and AP-1 mediated mechanism resulting in apoptosis [56, 57] indicating NQO-1 and HO-1 can also be activated through Nrf-2-independent mechanism upon high glucose treatment. Further, increased generation of ROS under high glucose conditions caused a loss in

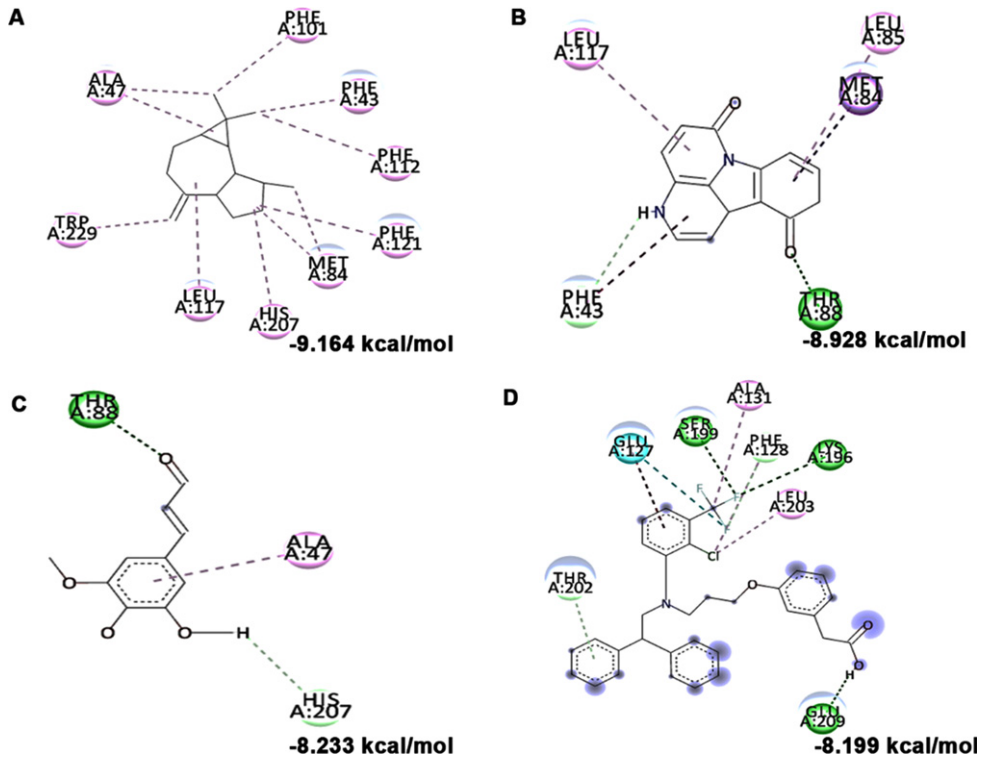


Fig. 13. Molecular docking and mode of interaction of compounds (top 3 hits) from HS extract against LXR- β (A) allo-Aromadendrene (B) 11-Hydroxycanthin-6-one (C) Sinapoyl aldehyde (D) GW3965 (Green indicates hydrogen bond, purple represents alkyl bond, pink represents π -alkyl bond)

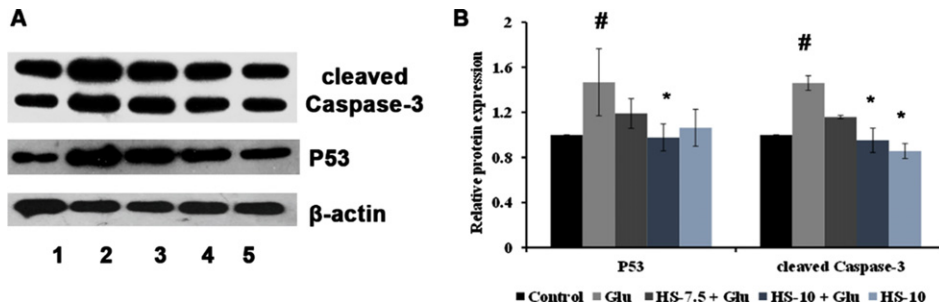


Fig. 14. (A) Representative blots showing the regulation of protein expression involved in apoptosis by HS extract (Lane: 1- Control; 2- High glucose; 3- HS-7.5 (pre-treatment 2 h) + high glucose; 4- HS-10 (pre-treatment 2 h) + high glucose; 5- HS-10) (B) Quantification of relative expression of P53 and Caspase-3 (Significance at $p < 0.05$; # Control vs High glucose; *High glucose vs HS pre-treated; $n = 3$).

$\Delta\Psi_m$ due to the opening of mitochondrial membrane permeability transition pore (mPTP) with increased expression of cyclophilin-D (Cyp-D), which is concomitant to the previous reports [58, 59]. Genetic ablation or blockade of Cyp-D has been reported to protect cells against various oxidative stress inducers through inhibition of mPTP [60, 61]. However, HS extract pre-treatment significantly protects the Neuro-2a cells against toxic insults by hampering ROS generation, inducing the expression of Nrf-2,

regulating the expression of antioxidant response elements (NQO-1, HO-1) and restoring $\Delta\Psi_m$ through the inhibition of Cyp-D.

Sirtuin-1 (SIRT-1) is involved in several cellular signaling, including ageing, stress response, and apoptosis. A noticeable reduction in SIRT-1 expression has been observed in cellular and experimental animals in response to diabetic and neurodegenerative conditions, implicating the protein's importance [62, 63]. The Forkhead family of transcription fac-

Table 3
Prediction of drug-likeness of selected compounds from HS by Lipinski's rule of five

Compounds	Molecular weight (≤ 500)	#H-bond acceptors (≤ 10)	#H-bond donors (≤ 5)	iLOGP (≤ 5)	Lipinski #violations (≤ 1)
Epigallocatechin 3-O-(3-O-methyl)gallate	472.4	11	7	2.23	2
11-Hydroxycanthin-6-one	236.23	2	1	1.81	0
N-Feruloyltyramine	313.35	4	3	2.58	0
Allo-Aromadendrene	204.35	0	0	3.26	1
Anisocoumarin H	314.38	4	1	3.42	0
Pelargonidin 3-glucoside	433.39	10	7	-2.09	1

Table 4
Toxicity prediction of phytochemicals from HS extract and BBB permeability

Compounds	Hepatotoxicity	Carcinogenicity	Immunotoxicity	Mutagenicity	Cytotoxicity	Predicted LD ₅₀ (mg/kg)	BBB permeability
Epigallocatechin 3-O-(3-O-methyl)gallate	-	-	+	-	-	1000	-
11-Hydroxycanthin-6-one	-	-	-	+	-	260	+
N-Feruloyltyramine	-	-	+	-	-	500	-
Allo-Aromadendrene	-	-	-	-	-	5000	+
Anisocoumarin H	-	-	-	-	-	3200	+
Pelargonidin 3-glucoside	-	-	-	-	-	5000	-

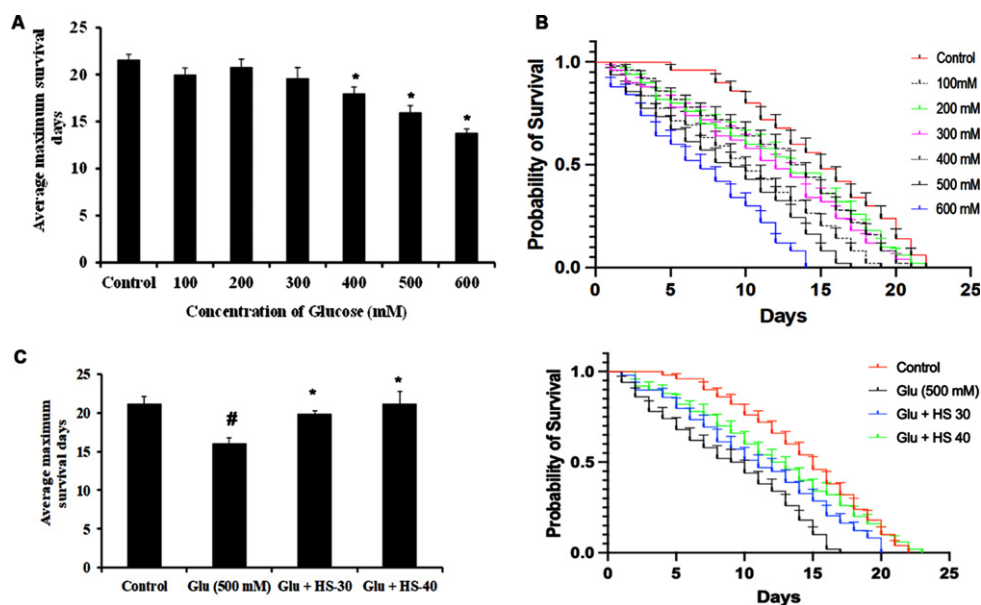


Fig. 15. HS extract extends lifespan in wild type nematodes against high glucose-induced toxicity (A) Glucose treatment in a dose-dependent manner reduced the average lifespan of N2 nematodes (B) Plots representing a reduction in life span in N2 nematodes upon treatment with glucose (100–600 mM) (C) HS extract increased the average lifespan of N2 worms against high glucose treatment (500 mM) (D) Plots showing lifespan extension of N2 worms by HS against high glucose (significance level at $p < 0.05$; # Controls vs high glucose; * High glucose vs HS treatment; $n = 5$)

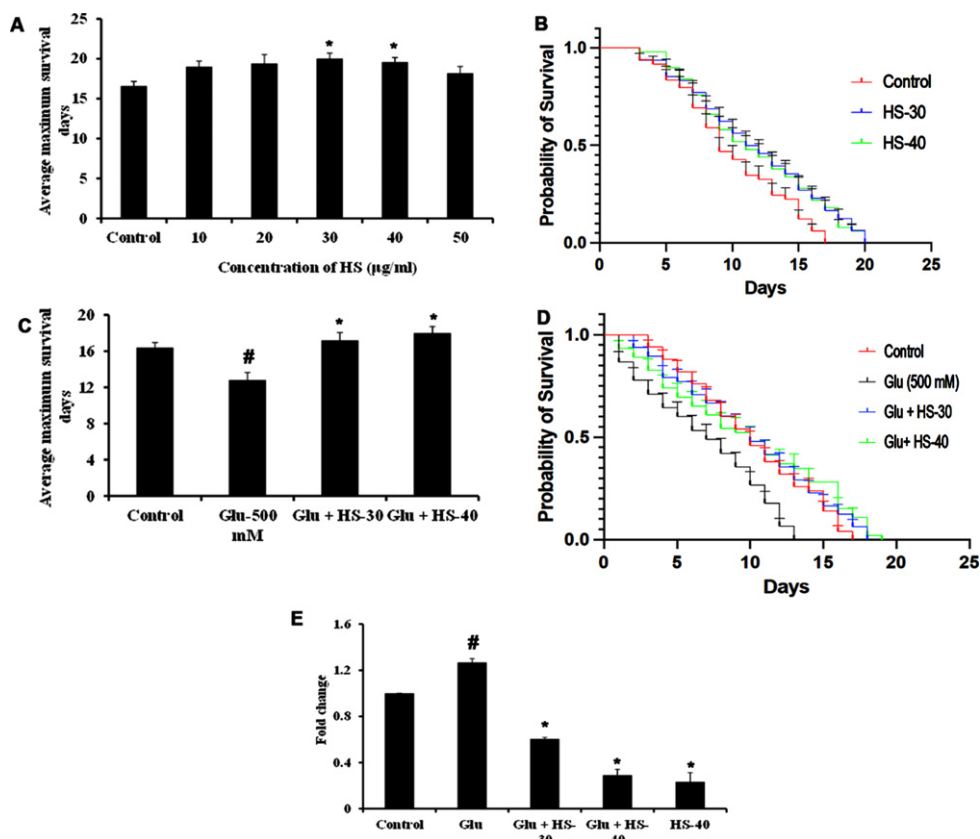


Fig. 16. HS extract extends lifespan in CL2006 transgenic strain against high glucose-induced toxicity (A) HS treatment in a dose-dependent manner increased the average lifespan of CL2006 strain (B) Plots showing life span extension by HS extract (30, 40 µg/ml) in CL2006 strain (C) HS extract increased the average lifespan of CL2006 worms against high glucose treatment (500 mM) (D) Plots showing lifespan extension of CL2006 worms by HS against high glucose (E) Inhibition of A β gene expression by HS extract (Significance at $p < 0.05$; # Controls vs high glucose; * High glucose vs HS treatment; $n = 5$).

tors, especially FOXO-1, is one of the downstream targets of SIRT-1, and the SIRT-1/FOXO-1 axis is reported to protect against oxidative stress. Previous studies have reported both the activation and suppression of FOXO-1 under high glucose-induced oxidative stress [63–65]. Although contradicting results have been observed under hyperglycemic conditions, it should be noted that short-term activation of FOXO-1 results in the increased expression of antioxidant defense enzymes to cope with the cellular stress, while long-term activation leads to cellular apoptotic pathways [66, 67]. In the current study, HS extract treatment increased the expression of SIRT-1 and downregulated FOXO-1 expression and protected Neuro-2a cells from high glucose-induced toxicity.

Evidence suggests that endoplasmic reticulum stress (ER stress) followed by unfolded protein response (UPR) occurs concomitantly with oxida-

tive stress conditions under chronic hyperglycemia [68]. The primary regulator of the UPR mechanism, Glucose-regulated protein 78 (GRP78), is upregulated in response to high glucose and evokes the expression of a series of transcription factors to cope with the cellular changes. The failure of this adaptive mechanism would result in the activation of the cell death pathway through the upregulation of C/EBP homologous protein/ growth arrest- and DNA damage-inducible gene 153 (CHOP/GADD153) [69]. The downregulation of Grp78 and CHOP has been reported to inhibit ER stress-induced cell death in diabetic rats and neurodegenerative conditions [40, 70]. In agreement with the previous reports, high glucose treatment induced the expression of Grp78 and CHOP and increased Calpain-1 and GSK-3 β expression, indicating ER stress. Calpain-1 activation has been associated with hyperglycemia-mediated apoptosis in various cellular models [71, 72]. In

addition, calpain-1 activates GSK-3 β and further contributes to insulin resistance and tau phosphorylation under diabetic and Alzheimer's conditions, respectively [73, 74]. GSK-3 β is also regulated by PI3K/AKT-mediated phosphorylation. Overactivation of GSK-3 β under disease conditions occurs with repression of AKT phosphorylation [75]. Downregulation of the AKT signaling pathway has been observed under hyperglycemic conditions in cellular models [76, 77]. In the current study, it can also be observed that there is a significant reduction in p-AKT/AKT under high glucose treatment, which could be due to the increase in ROS levels corroborating with the earlier reports and pre-treatment with HS extract reversed the effect to offer neuroprotection.

The activation of the JNK signaling pathway also follows the ER stress in cells. It is associated with cell death, and inhibition of JNK phosphorylation has been reported as a mechanism to protect cells against high glucose-induced toxicity [78, 79]. Further, glucose-induced JNK activation causes abnormality in glucose metabolism and lipid accumulation through the repression of Liver X receptors (LXRs). The LXRs belong to the nuclear receptor superfamily and regulate the activation of several transcription factors involved in cholesterol and lipid metabolism [80]. In addition, LXRs activation was reported to regulate the abundance of lipid rafts within the plasma membrane enriched with cholesterol and several cell signaling proteins [81, 82]. High glucose-mediated hampering of cholesterol biosynthesis has been found to disrupt lipid raft stability in INS-1 β -cells causing diabetic complications and inducing β -secretase-mediated A β production through the reorganization of lipid raft coupled with LXR downregulation in SK-N-MC cells, causing neurodegeneration [83–85]. Experimental evidence shows an inverse correlation between JNK phosphorylation, LXR activation, and LXR agonist TO901317 to suppress ROS-mediated JNK phosphorylation and activate the AKT pathway in diabetic mice and SK-N-MC cells treated with high glucose [85, 86]. Further, the downstream targets of LXRs, including ATP-binding cassette transporter A1 (ABCA-1), Seladin-1 that are involved in cholesterol export and maintaining lipid raft integrity, were also downregulated under hyperglycemic conditions causing perturbations in cholesterol homeostasis and lipid raft integrity [87, 88]. Akt can also activate Seladin-1 under stress stimuli and exhibits pro-survival effects to offer neuroprotection [89, 90]. In the current study, high glucose treatment induced JNK phosphorylation followed by repression of

LXRs and the downstream targets Seladin-1, ABCA-1 to disrupt cholesterol homeostasis. However, HS pre-treatment significantly reversed the effect and protected the cells from neurodegeneration.

Further, JNK activation can also induce the expression of the tumor suppressor protein to induce apoptosis against high glucose conditions [91, 92]. In addition to JNK, ER-stress associated GSK-3 β activation also induces the expression of p53 and caspase-3 to promote apoptosis [93–95]. Corroborating the previous reports, high glucose treatment in Neuro-2a cells induced apoptosis through the upregulation of p53 and cleaved caspase-3. However, HS pre-treatment protected the cells by significantly downregulating the expression of apoptotic proteins and offered neuroprotection.

In addition to the *in vitro* studies with Neuro-2a cells, the simple nematode model system *C. elegans* were also used to substantiate the findings. We have used the wild type strain N2 and the transgenic strain CL2006, expressing A β (a model for studying AD pathogenesis). The transgenic strain CL2006, constitutively expresses human A β _{3–42} in the body wall muscle cells and exhibits age-related paralysis and reduced survival, which is related to the accumulation of A β _{3–42} fibrils and oligomers [28]. Previously, we have reported the anti-ageing properties of HS extract in wild type *C. elegans* [40]. Preliminary studies have reported the reduction in lifespan in *C. elegans* upon high glucose treatment [96, 97]. High glucose treatment in transgenic strains expressing A β and tau has been reported to further exacerbate the condition, coupled with an increase in paralysis and impairment in acetylcholine neurotransmission [98]. In line with the reports, high glucose reduced the lifespan of *C. elegans* (both N2 and CL2006 strain) and further induced the expression of A β . At the same time, HS treatment significantly extended the lifespan and suppressed the expression of A β in response to high glucose treatment. Our results show that the HS extract offers neuroprotection under hyperglycemic conditions by modulating critical pathways involved in the progression of the disease.

LC-MS/MS analysis of the ethanol extract of HS revealed several bioactive compounds, including Hibiscus acid, Hibiscus acid hydroxyethylester, Epigallocatechin 3-O-(3-O-methylgallate), 3',4',7-Trihydroxyisoflavan, 11-Hydroxycanthin-6-one, Pelargonidin 3-rhamnoside 5-glucoside, Glucovanillin, Anisocoumarin H, Isobetanin, allo-Aromadendrene, 3-dehydroquinone and so on. Previous studies have reported on the antioxidant,

anti-diabetic and neuroprotective effects of some of the phytochemicals identified from HS. In silico docking approach, which is one of the powerful tools in drug design, was employed with the identified compounds against potential protein targets to substantiate the obtained results. Herein, blind docking was performed to identify potential binding sites through several trials and energy calculations by searching the entire surface of the protein target. Pioneering studies have indicated that apart from the primary binding sites, there occurs biologically relevant secondary binding sites and the addition of small molecules to such sites could modulate the function of the protein. In this regard, in our current study we have employed blind docking, which is considered to be unbiased as it scans the entire structure of the protein for finding out the putative binding site of ligand [99–101]. Among the identified compounds, allo-Aromadendrene, 11-Hydroxycanthin-6-one, Sinapoyl aldehyde, Pelargonidin 3-rhamnoside 5-glucoside, Anisocoumarin H and N-Feruloyltyramine have been repeatedly found to have a high binding affinity with the various target proteins through covalent hydrogen bond, alkyl bonds, π -sulfur bond and π -alkyl bond. Hydrogen interactions help to stabilize the target protein and ligand binding and bring them into proximity, alkyl and π -alkyl bonds help in improving the hydrophobic interaction of the tested compounds in the binding pocket of the protein, while π -sulfur interactions help in the intercalation of the tested compounds in the binding site [102, 103]. In addition, ADMET analysis showed that most of the bioactive compounds fit into the Lipinski's rule of five and are devoid of hepatotoxicity and carcinogenicity.

Moreover, Pelargonidin has been reported to ameliorate oxidative stress in HepG2 cells, improve memory deficit in the AD rat model, and ameliorate diabetic neuropathy in rats [104–106]. The red-beet betalain pigments containing isobetanin inhibit A β aggregation and toxicity in the AD transgenic *C. elegans* model [107]. Various *in vitro* and *in vivo* studies have reported on the mechanism of chlorogenic acid to ameliorate diabetes [108]. The essential oil Alloaromadendrene was shown to extend the lifespan of *C. elegans* [109]. Canthin-6-one alkaloid exhibited a neuroprotective effect against glutamate and A β ₂₅₋₃₅ induced toxicity and showed an anti-diabetic effect in rats [110, 111]. N-feruloyltyramine exhibited antioxidant properties and protected L02 cells from H₂O₂-mediated oxidative damages [112]. The

reports indicate that these compounds' individual or combinatorial effects could be responsible for the observed neuroprotective effect. However, other factors, including oral bioavailability, toxicity and blood brain permeability of the compounds are required to be tested in animal models to claim the individual compounds' neuroprotective effect. In addition, one of the limitations pertaining the current study is the physiological relevance of the used *in vitro* model. Although, Neuro-2a cells offer a significant platform for the pre-clinical investigation of the effects of drugs against any neurological diseases and help in the identification of mechanistic pathways of drug candidates, the supraphysiological dosages, and lack of physiologically relevant microenvironment acts as a major hindrance while translating the applicability of the obtained data to clinical trials. Hence, studies with 3D neuronal cultures, or higher model organisms must be performed with HS extract before inferring to the therapeutic application of HS against AD associated with diabetes.

5. Conclusion

Overall, the ethanol extract of the red calyces of HS exhibits a neuroprotective effect against high glucose-induced through regulating genes and proteins involved in stress response and cellular signaling. Further, high glucose-mediated reduction in lifespan was reversed through the inhibition of A β expression. Our results propose that HS with its active constituents, including allo-Aromadendrene, Anisocoumarin H, and N-Feruloyltyramine can be considered promising therapeutic agents to treat hyperglycemia associated neurodegenerative diseases. As, HS has been already reported to be safe to consume in human, further studies on individual compounds identified, as well as the formulation of extract and testing in higher model system or the elderly individuals with AD might prove beneficial in the treatment/management of neurodegenerative diseases.

Acknowledgments

DSM wishes to thank the Second Century Fund (C2F) for Postdoctoral Fellowship, Chulalongkorn University, Thailand, for the support. MIP and JMB wish to thank the Ratchadaphiseksomphot

Endowment Fund for Postdoctoral Fellowship, Chulalongkorn University.

Funding

The present work was supported by Natural Products for Neuroprotection and Anti-ageing Research Unit.

Conflicts of interest

The authors declare no conflict of interest.

References

- [1] Fan HC, Chi CS, Cheng SN, Lee HF, Tsai JD, Lin SZ, Harn HJ. Targeting new candidate genes by small molecules approaching neurodegenerative diseases. *Int J Mol Sci*. 2015;17(1):26.
- [2] Hou YC, Chao PD, Chen SY. Honokiol and magnolol increased hippocampal acetylcholine release in freely-moving rats. *Am J Chin Med*. 2000;28(3-4):379-84.
- [3] Babizhayev MA, Stokov IA, Nosikov VV, Savel'yeva EL, Sitnikov VF, Yegorov YE, Lankin VZ. The role of oxidative stress in diabetic neuropathy: Generation of free radical species in the glycation reaction and gene polymorphisms encoding antioxidant enzymes to genetic susceptibility to diabetic neuropathy in population of type I diabetic patients. *Cell Biochem Biophys*. 2015;71(3):1425-43.
- [4] Luo X, Wu J, Jing S, Yan LJ. Hyperglycemic stress and carbon stress in diabetic glucotoxicity. *Aging Dis*. 2016;7(1):90-110.
- [5] Peila R, Rodriguez BL, White LR, Launer LJ. Fasting insulin and incident dementia in an elderly population of Japanese-American men. *Neurology*. 2004;63(2):228-33.
- [6] Peila R, Rodriguez BL, Launer LJ; Honolulu-Asia Aging Study. Type 2 diabetes, APOE gene, and the risk for dementia and related pathologies: The Honolulu-Asia Aging Study. *Diabetes*. 2002;51(4):1256-62.
- [7] Arvanitakis Z, Wilson RS, Bienias JL, Evans DA, Bennett DA. Diabetes mellitus and risk of Alzheimer disease and decline in cognitive function. *Arch Neurol*. 2004;61(5):661-6.
- [8] Ott A, Stolk RP, van Harskamp F, Pols HA, Hofman A, Breteler MM. Diabetes mellitus and the risk of dementia: The Rotterdam Study. *Neurology*. 1999;53(9):1937-42.
- [9] Macauley SL, Stanley M, Caesar EE, Yamada SA, Raichle ME, Perez R, Mahan TE, Sutphen CL, Holtzman DM. Hyperglycemia modulates extracellular amyloid- β concentrations and neuronal activity *in vivo*. *J Clin Invest*. 2015;125(6):2463-7.
- [10] Yang Y, Wu Y, Zhang S, Song W. High glucose promotes A β production by inhibiting APP degradation. *PLoS One*. 2013;8(7):e69824.
- [11] Lee HJ, Ryu JM, Jung YH, Lee SJ, Kim JY, Lee SH, Hwang IK, Seong JK, Han HJ. High glucose upregulates BACE1-mediated A β production through ROS-dependent HIF-1 α and LXR α /ABCA1-regulated lipid raft reorganization in SK-N-MC cells. *Sci Rep*. 2016;6:36746.
- [12] Jolivald CG, Lee CA, Beiswenger KK, Smith JL, Orlov M, Torrance MA, Masliah E. Defective insulin signaling pathway and increased glycogen synthase kinase-3 activity in the brain of diabetic mice: Parallels with Alzheimer's disease and correction by insulin. *J Neurosci Res*. 2008;86(15):3265-74.
- [13] Kim DJ, Yu JH, Shin MS, Shin YW, Kim MS. Hyperglycemia reduces efficiency of brain networks in subjects with type 2 diabetes. *PLoS One*. 2016;11(6):e0157268.
- [14] Lv YQ, Yuan L, Sun Y, Dou HW, Su JH, Hou ZP, Li JY, Li W. Long-term hyperglycemia aggravates α -synuclein aggregation and dopaminergic neuronal loss in a Parkinson's disease mouse model. *Transl Neurodegener*. 2022;11(1):14.
- [15] Wu J, Zhou SL, Pi LH, Shi XJ, Ma LR, Chen Z, Qu ML, Li X, Nie SD, Liao DF, Pei JJ, Wang S. High glucose induces formation of tau hyperphosphorylation via Cav-1-mTOR pathway: A potential molecular mechanism for diabetes-induced cognitive dysfunction. *Oncotarget*. 2017;8(25):40843-56.
- [16] Lu XY, Huang S, Chen QB, et al. Metformin ameliorates A β pathology by insulin-degrading enzyme in a transgenic mouse model of Alzheimer's disease. *Oxid Med Cell Longev*. 2020;2020:2315106.
- [17] Shi Q, Liu S, Fonseca VA, Thethi TK, Shi L. Effect of metformin on neurodegenerative disease among elderly adult US veterans with type 2 diabetes mellitus. *BMJ Open*. 2019;9(7):e024954. doi: 10.1136/bmjopen-2018-024954. PMID: 31366635; PMCID: PMC6677947.
- [18] Ma L, Shao Z, Wang R, Zhao Z, Dong W, Zhang J, Zhang X, Sheng S, Ji Z, Zhang J. Rosiglitazone improves learning and memory ability in rats with type 2 diabetes through the insulin signaling pathway. *Am J Med Sci*. 2015;350(2):121-8. doi: 10.1097/MAJ.000000000000499. PMID: 25973687.
- [19] Batista AF, Forny-Germano L, Clarke JR, Lyra E Silva NM, Brito-Moreira J, Boehnke SE, Winterborn A, Coe BC, Lablans A, Vital JF, Marques SA, Martinez AM, Gralle M, Holscher C, Klein WL, Houzel JC, Ferreira ST, Munoz DP, De Felice FG. The diabetes drug liraglutide reverses cognitive impairment in mice and attenuates insulin receptor and synaptic pathology in a non-human primate model of Alzheimer's disease. *J Pathol*. 2018;245(1):85-100. doi: 10.1002/path.5056. Epub 2018 Apr 2. PMID: 29435980; PMCID: PMC5947670.
- [20] Wang X, Wang L, Xu Y, et al. Intranasal administration of Exendin-4 antagonizes A β 31-35-induced disruption of circadian rhythm and impairment of learning and memory. *Aging Clin Exp Res*. 2016;28;1259-66. <https://doi.org/10.1007/s40520-016-0548-z>
- [21] Yang S, Chen Z, Cao M, Li R, Wang Z, Zhang M. Pioglitazone ameliorates A β 42 deposition in rats with diet-induced insulin resistance associated with AKT/GSK3 β activation. *Mol Med Rep*. 2017;15(5):2588-94. doi: 10.3892/mmr.2017.6342. Epub 2017 Mar 16. PMID: 28447730; PMCID: PMC5428924.

- [22] Jung KI, Han JS, Park CK. Neuroprotective effects of nicotinamide (Vitamin B3) on neurodegeneration in diabetic rat retinas. *Nutrients*. 2022;14(6):1162.
- [23] Peng D, Xia Q, Guan L, Li HY, Qiao LJ, Chen YB, Cai YF, Wang Q, Zhang SJ. Carnosine improves cognitive impairment through promoting SIRT6 expression and inhibiting endoplasmic reticulum stress in a diabetic encephalopathy model. *Rejuvenation Res*. 2022;25(2):79-88.
- [24] El-Feky AM, Elbatany MM, Aboul Naser AF, Younis EA, Hamed MA. *Salvia hispanica* L. seeds extract alleviate encephalopathy in streptozotocin-induced diabetes in rats: Role of oxidative stress, neurotransmitters, DNA and histological indices. *Biomarkers*. 2022;15:1-14.
- [25] Lupaescu AV, Iavorschi M, Covasa M. The use of bioactive compounds in hyperglycemia- and amyloid fibrils-induced toxicity in type 2 diabetes and Alzheimer's disease. *Pharmaceutics*. 2022;14(2):235.
- [26] Alkharfy KM, Ahmad A, Siddiquei MM, Ghulam M, El-Asrar AA. Thymoquinone attenuates retinal expression of mediators and markers of neurodegeneration in a diabetic animal model. *Curr Mol Pharmacol*. 2022. doi: 10.2174/1874467215666220113105300.
- [27] Alvarez J, Alvarez-Illera P, Santo-Domingo J, Fonteriz RI, Montero M. Modeling Alzheimer's disease in *Caenorhabditis elegans*. *Biomedicines*. 2022;10:288.
- [28] Malar DS, Prasanth MI, Jeyakumar M, Balamurugan K, Devi KP. Vitexin prevents A β proteotoxicity in transgenic *Caenorhabditis elegans* model of Alzheimer's disease by modulating unfolded protein response. *J Biochem Mol Toxicol*. 2021;35:e22632.
- [29] Alexander AG, Marfil V, Li C. Use of *Caenorhabditis elegans* as a model to study Alzheimer's disease and other neurodegenerative diseases. *Front Genet*. 2014;5:279.
- [30] Di Carlo M. Simple model systems: A challenge for Alzheimer's disease. *Immun Ageing*. 2012;9:3.
- [31] Amer SA, Al-Khalafah HS, Gouda A, Osman A, Goda NIA, Mohammed HA, Darwish MIM, Hassan AM, Mohamed SKA. Potential effects of anthocyanin-rich roselle (*Hibiscus sabdariffa* L.) extract on the growth, intestinal histomorphology, blood biochemical parameters, and the immune status of broiler chickens. *Antioxidants (Basel)*. 2022;11(3):544.
- [32] Khan NH, Abdulbaqi IM, Darwis Y, Aminu N, Chan SY. A stability-indicating HPLC-UV method for the quantification of anthocyanin in Roselle (*Hibiscus Sabdariffa* L.) spray-dried extract, oral powder, and lozenges. *Heliyon*. 2022;8(3):e09177.
- [33] Patel S. *Hibiscus sabdariffa*: An ideal yet under-exploited candidate for nutraceutical applications. *Biomed Prev Nutr*. 2014;4(1):23-7.
- [34] Mayasari NR, Susetyowati, Wahyuningsih MSH, Probosuseno. Antidiabetic effect of rosella-stevia tea on prediabetic women in Yogyakarta, Indonesia. *J Am Coll Nutr*. 2018;37(5):373-9.
- [35] Serna A, Marhuenda J, Arcusa R, Pérez-Piñero S, Sánchez-Macarro M, García-Muñoz AM, Victoria-Montesinos D, Cánovas F, López-Román FJ. Effectiveness of a polyphenolic extract (*Lippia citriodora* and *Hibiscus sabdariffa*) on appetite regulation in overweight and obese grade I population: An 8-week randomized, double-blind, crossover, placebo-controlled trial. *Eur J Nutr*. 2022;61(2): 825-41.
- [36] Diantini A, Rahmat S, Alpiani A, Sumiwi SA, Lubis L, Levita J. Effect of the roselle (*Hibiscus sabdariffa* L.) calyces drink on the physiological parameters of healthy adult subjects. *Biomed Rep*. 2021;15(5):89.
- [37] Peng CH, Chyau CC, Chan KC, Chan TH, Wang CJ, Huang CN. *Hibiscus sabdariffa* polyphenolic extract inhibits hyperglycemia, hyperlipidemia, and glycation-oxidative stress while improving insulin resistance. *J Agric Food Chem*. 2011;59(18):9901-9.
- [38] Mishra MK, Wang J, Mirzaei R, Chan R, Melo H, Zhang P, Ling CC, Bruccoleri A, Tang L, Yong VW. A distinct *Hibiscus sabdariffa* extract prevents iron neurotoxicity, a driver of multiple sclerosis pathology. *Cells*. 2022;11(3): 440.
- [39] Seung TW, Park SK, Kang JY, Kim JM, Park SH, Kwon BS, Lee CJ, Kang JE, Kim DO, Lee U, Heo HJ. Ethyl acetate fraction from *Hibiscus sabdariffa* L. attenuates diabetes-associated cognitive impairment in mice. *Food Res Int*. 2018;105:589-98.
- [40] Malar DS, Prasanth MI, Brimson JM, Verma K, Prasansuklab A, Tencomnao T. *Hibiscus sabdariffa* extract protects HT-22 cells from glutamate-induced neurodegeneration by upregulating glutamate transporters and exerts lifespan extension in *C. Elegans* via DAF-16 mediated pathway. *Nutr Healthy Aging*. 2021;6(3):229-47.
- [41] Ellman GL, Courtney KD, Andres V Jr, Feather-Stone RM. A new and rapid colorimetric determination of acetylcholinesterase activity. *Biochem Pharmacol*. 1961;7:88-95.
- [42] Malar DS, Prasanth, MI, Shafreen RB, Balamurugan K, Devi KP. *Grewia tiliaefolia* and its active compound vitexin regulate the expression of glutamate transporters and protect Neuro-2a cells from glutamate toxicity. *Life Sci*. 2018;203:233-41.
- [43] Malar DS, Suryanarayanan V, Prasanth MI, Singh SK, Balamurugan K, Devi KP. Vitexin inhibits A β 25-35 induced toxicity in Neuro-2a cells by augmenting Nrf-2/HO-1 dependent antioxidant pathway and regulating lipid homeostasis by the activation of LXR- α . *Toxicol In Vitro*. 2018;50:160-71.
- [44] Guex N, Peitsch MC. Swiss-PdbViewer: A fast and easy-to-use PDB viewer for Macintosh and PC. *Protein Data Bank Quarterly Newsletter*. 1996;77:7.
- [45] Verma K, Lahariya AK, Dubey S, Verma AK, Das A, Schneider KA, Bharti PK. An integrated virtual screening and drug repurposing strategy for the discovery of new antimalarial drugs against *Plasmodium falciparum* phosphatidylinositol 3-kinase. *J Cell Biochem*. 2021;122(10):1326-36.
- [46] Banerjee P, Eckert AO, Schrey AK, Preissner R. ProTox-II: A webserver for the prediction of toxicity of chemicals. *Nucleic Acids Res*. 2018;46(W1):W257-63.
- [47] Verma K, Kannan K, V S, R S, V K, K R. Exploring β -tubulin inhibitors from plant origin using computational approach. *Phytochem Anal*. 2017;28:230-41.
- [48] Prasanth MI, Brimson JM, Malar DS, Prasansuklab A, Tencomnao T. *Streblus asper* Lour. Exerts MAPK and SKN-1 mediated anti-aging, anti-photoaging activities and imparts neuroprotection by ameliorating A β in *Caenorhabditis elegans*. *Nutr Healthy Aging*. 2021;6(3):211-27.
- [49] Prasanth MI, Brimson JM, Chuchawankul S, Sukprasansap M, Tencomnao T. Antiaging, stress resistance, and neuroprotective efficacies of *Cleistocalyx nervosum* var. *paniala*

- fruit extracts using *Caenorhabditis elegans* model. *Oxid Med Cell Longev*. 2019;2019:7024785.
- [50] Zhang S, Xue R, Hu R. The neuroprotective effect and action mechanism of polyphenols in diabetes mellitus-related cognitive dysfunction. *Eur J Nutr*. 2020;59(4):1295-311.
- [51] Capiotti KM, De Moraes DA, Menezes FP, Kist LW, Bogo MR, Da Silva RS. Hyperglycemia induces memory impairment linked to increased acetylcholinesterase activity in zebrafish (*Danio rerio*). *Behav Brain Res*. 2014;274:319-25.
- [52] Song J, Lee B, Kang S, Oh Y, Kim E, Kim CH, Song HT, Lee JE. Agmatine ameliorates high glucose-induced neuronal cell senescence by regulating the p21 and p53 signaling. *Exp Neurobiol*. 2016;25(1):24-32.
- [53] Albert-Garay JS, Riesgo-Escovar JR, Salceda R. High glucose concentrations induce oxidative stress by inhibiting Nrf2 expression in rat Müller retinal cells *in vitro*. *Sci Rep*. 2022;12(1):1261.
- [54] Sykietis GP, Bohmann D. Stress-activated cap'n'collar transcription factors in aging and human disease. *Sci Signal*. 2010;3(112):re3.
- [55] Hayes JD, Dinkova-Kostova AT. The Nrf2 regulatory network provides an interface between redox and intermediary metabolism. *Trends Biochem Sci*. 2014;39(4):199-218.
- [56] Yang CM, Lin CC, Hsieh HL. High-glucose-derived oxidative stress-dependent heme oxygenase-1 expression from astrocytes contributes to the neuronal apoptosis. *Mol Neurobiol*. 2017;54(1):470-83.
- [57] He M, Pan H, Xiao C, Pu M. Roles for redox signaling by NADPH oxidase in hyperglycemia-induced heme oxygenase-1 expression in the diabetic retina. *Invest Ophthalmol Vis Sci*. 2013;54(6):4092-101.
- [58] Yu T, Robotham JL, Yoon Y. Increased production of reactive oxygen species in hyperglycemic conditions requires dynamic change of mitochondrial morphology. *Proc Natl Acad Sci U S A*. 2006;103(8):2653-8.
- [59] Trudeau K, Molina AJ, Roy S. High glucose induces mitochondrial morphology and metabolic changes in retinal pericytes. *Invest Ophthalmol Vis Sci*. 2011;52(12):8657-64.
- [60] Huang S, Zheng B, Jin X, Yu Q, Zhang X, Sun X, Chen Y, Ren X, Wismeijer D, Ma J, Zhang C, Wu G, Pan Y. Blockade of cyclophilin D attenuates oxidative stress-induced cell death in human dental pulp cells. *Oxid Med Cell Longev*. 2019;2019:1729013.
- [61] Devalaraja-Narashimha K, Diener AM, Padanilam BJ. Cyclophilin D gene ablation protects mice from ischemic renal injury. *Am J Physiol Renal Physiol*. 2009;297(3):F749-59.
- [62] Shi X, Pi L, Zhou S, Li X, Min F, Wang S, Liu Z, Wu J. Activation of sirtuin 1 attenuates high glucose-induced neuronal apoptosis by deacetylating p53. *Front Endocrinol (Lausanne)*. 2018;9:274.
- [63] Ren BC, Zhang YF, Liu SS, Cheng XJ, Yang X, Cui XG, Zhao XR, Zhao H, Hao MF, Li MD, Tie YY, Qu L, Li XY. Curcumin alleviates oxidative stress and inhibits apoptosis in diabetic cardiomyopathy via Sirt1-Foxo1 and PI3K-Akt signalling pathways. *J Cell Mol Med*. 2020;24(21):12355-67.
- [64] Marchetti V, Menghini R, Rizza S, Vivanti A, Feccia T, Lauro D, Fukamizu A, Lauro R, Federici M. Benfotiamine counteracts glucose toxicity effects on endothelial progenitor cell differentiation via Akt/FoxO signaling. *Diabetes*. 2006;55(8):2231-7.
- [65] Zhang Q, Wang C, Tang Y, Zhu Q, Li Y, Chen H, Bao Y, Xue S, Sun L, Tang W, Chen X, Shi Y, Qu L, Lu B, Zheng J. High glucose upregulates osteopontin expression by FoxO1 activation in macrophages. *J Endocrinol*. 2019;242(2):51-64.
- [66] Martinez SC, Tanabe K, Cras-Meneur C, Abumrad NA, Bernal-Mizrachi E, Permutt MA. Inhibition of Foxo1 protects pancreatic islet beta-cells against fatty acid and endoplasmic reticulum stress-induced apoptosis. *Diabetes*. 2008;57:846-59.
- [67] Manolopoulos KN, Klotz LO, Korsten P, Bornstein SR, Barthel A. Linking Alzheimer's disease to insulin resistance: The FoxO response to oxidative stress. *Mol Psychiatry*. 2010;15(11):1046-52.
- [68] Cao Y, Hao Y, Li H, Liu Q, Gao F, Liu W, Duan H. Role of endoplasmic reticulum stress in apoptosis of differentiated mouse podocytes induced by high glucose. *Int J Mol Med*. 2014;33(4):809-16.
- [69] Yang Y, Liu L, Naik I, Braunstein Z, Zhong J, Ren B. Transcription factor C/EBP homologous protein in health and diseases. *Front Immunol*. 2017;8:1612.
- [70] Chen Y, Gui D, Chen J, He D, Luo Y, Wang N. Down-regulation of PERK-ATF4-CHOP pathway by Astragaloside IV is associated with the inhibition of endoplasmic reticulum stress-induced podocyte apoptosis in diabetic rats. *Cell Physiol Biochem*. 2014;33(6):1975-87.
- [71] Li Y, Li Y, Feng Q, Arnold M, Peng T. Calpain activation contributes to hyperglycaemia-induced apoptosis in cardiomyocytes. *Cardiovasc Res*. 2009;84(1):100-10.
- [72] Tie L, Xu Y, Lin YH, Yao XH, Wu HL, Li YH, Shen ZF, Yu HM, Li XJ. Down-regulation of brain-pancreas relative protein in diabetic rats and by high glucose in PC12 cells: Prevention by calpain inhibitors. *J Pharmacol Sci*. 2008;106(1):28-37.
- [73] Leng S, Zhang W, Zheng Y, Liberman Z, Rhodes CJ, Eldar-Finkelman H, Sun XJ. Glycogen synthase kinase 3 beta mediates high glucose-induced ubiquitination and proteasome degradation of insulin receptor substrate 1. *J Endocrinol*. 2010;206(2):171-81.
- [74] Jin N, Yin X, Yu D, Cao M, Gong CX, Iqbal K, Ding F, Gu X, Liu F. Truncation and activation of GSK-3 β by calpain I: A molecular mechanism links to tau hyperphosphorylation in Alzheimer's Disease. *Sci Rep*. 2015;5:8187.
- [75] Endo H, Nito C, Kamada H, Nishi T, Chan PH. Activation of the Akt/GSK3beta signaling pathway mediates survival of vulnerable hippocampal neurons after transient global cerebral ischemia in rats. *J Cereb Blood Flow Metab*. 2006;26(12):1479-89.
- [76] Huang X, Liu G, Guo J, Su Z. The PI3K/AKT pathway in obesity and type 2 diabetes. *Int J Biol Sci*. 2018;14(11):1483-96.
- [77] Qin D, Zhang GM, Xu X, Wang LY. The PI3K/Akt signaling pathway mediates the high glucose-induced expression of extracellular matrix molecules in human retinal pigment epithelial cells. *J Diabetes Res*. 2015;2015:920280.
- [78] Zhou J, Deo BK, Hosoya K, Terasaki T, Obrosova IG, Brosius FC 3rd, Kumagai AK. Increased JNK phosphorylation and oxidative stress in response to increased glucose

- flux through increased GLUT1 expression in rat retinal endothelial cells. *Invest Ophthalmol Vis Sci.* 2005;46(9):3403-10.
- [79] Oshitari T, Bikbova G, Yamamoto S. Increased expression of phosphorylated c-Jun and phosphorylated c-Jun N-terminal kinase associated with neuronal cell death in diabetic and high glucose exposed rat retinas. *Brain Res Bull.* 2014;101:18-25.
- [80] Bilotta MT, Petillo S, Santoni A, Cippitelli M. Liver X receptors: Regulators of cholesterol metabolism, inflammation, autoimmunity, and cancer. *Front Immunol.* 2020;11:584303.
- [81] Bickel PE. Lipid rafts and insulin signaling. *Am J Physiol Endocrinol Metab.* 2002;282(1):E1-10.
- [82] Sviridov D, Mukhamedova N, Miller YI. Lipid rafts as a therapeutic target. *J Lipid Res.* 2020;61(5):687-95.
- [83] Somanath S, Barg S, Marshall C, Silwood CJ, Turner MD. High extracellular glucose inhibits exocytosis through disruption of syntaxin 1A-containing lipid rafts. *Biochem Biophys Res Commun.* 2009;389(2):241-6.
- [84] Chentouf M, Guzman C, Hamze M, Gross R, Lajoix AD, Peraldi-Roux S. Possible protective effect of membrane lipid rafts against interleukin-1 β -mediated anti-proliferative effect in INS-1 cells. *PLoS One.* 2014;9(7):e102889.
- [85] Lee HJ, Ryu JM, Jung YH, Lee SJ, Kim JY, Lee SH, Hwang IK, Seong JK, Han HJ. High glucose upregulates BACE1-mediated A β production through ROS-dependent HIF-1 α and LXR α /ABCA1-regulated lipid raft reorganization in SK-N-MC cells. *Sci Rep.* 2016;6:36746.
- [86] Dong Y, Gao G, Fan H, Li S, Li X, Liu W. Activation of the liver X receptor by agonist TO901317 improves hepatic insulin resistance via suppressing reactive oxygen species and JNK pathway. *PLoS One.* 2015;10(4):e0124778.
- [87] Hussein MA, Shrestha E, Ouimet M, Barrett TJ, Leone S, Moore KJ, Hérault Y, Fisher EA, Garabedian MJ. LXR-mediated ABCA1 expression and function are modulated by high glucose and PRMT2. *PLoS One.* 2015;10(8):e0135218.
- [88] Kazkayasi I, Ismail MA, Parrado-Fernandez C, Björkhem I, Pekiner C, Uma S, Cedazo-Minguez A, Burul-Bozkurt N. Lack of insulin results in reduced seladin-1 expression in primary cultured neurons and in cerebral cortex of STZ-induced diabetic rats. *Neurosci Lett.* 2016;633:174-81.
- [89] Hwang SL, Lin JA, Shih PH, Yeh CT, Yen GC. Procellular survival and neuroprotection of citrus flavonoid: The actions of hesperetin in PC12 cells. *Food Funct.* 2012;3(10):1082-90.
- [90] Bing L, Wu J, Zhang J, Chen Y, Hong Z, Zu H. DHT inhibits the A β 25-35-induced apoptosis by regulation of seladin-1, survivin, XIAP, bax, and bcl-xl expression through a rapid PI3-K/Akt signaling in C6 glial cell lines. *Neurochem Res.* 2015;40(1):41-8.
- [91] Oleinik NV, Krupenko NI, Krupenko SA. Cooperation between JNK1 and JNK2 in activation of p53 apoptotic pathway. *Oncogene.* 2007;26(51):7222-30.
- [92] Wu Y, Lee S, Bobadilla S, Duan SZ, Liu X. High glucose-induced p53 phosphorylation contributes to impairment of endothelial antioxidant system. *Biochim Biophys Acta Mol Basis Dis.* 2017;1863(9):2355-62.
- [93] Thotala DK, Hallahan DE, Yazlovitskaya EM. Glycogen synthase kinase 3 β inhibitors protect hippocampal neurons from radiation-induced apoptosis by regulating MDM2-p53 pathway. *Cell Death Differ.* 2012;19(3):387-96.
- [94] Bhat RV, Leonov S, Luthman J, Scott CW, Lee CM. Interactions between GSK3 β and caspase signalling pathways during NGF deprivation induced cell death. *J Alzheimers Dis.* 2002;4(4):291-301.
- [95] Song L, De Sarno P, Jope RS. Central role of glycogen synthase kinase-3 β in endoplasmic reticulum stress-induced caspase-3 activation. *J Biol Chem.* 2002;277(47):44701-8.
- [96] Alcántar-Fernández J, González-Maciel A, Reynoso-Robles R, Pérez Andrade ME, Hernández-Vázquez AJ, Velázquez-Arellano A, Miranda-Ríos J. High-glucose diets induce mitochondrial dysfunction in *Caenorhabditis elegans*. *PLoS One.* 2019;14(12):e0226652.
- [97] Alcántar-Fernández J, Navarro RE, Salazar-Martínez AM, Pérez-Andrade ME, Miranda-Ríos J. *Caenorhabditis elegans* respond to high-glucose diets through a network of stress-responsive transcription factors. *PLoS One.* 2018;13(7):e0199888.
- [98] Ahmad W. Glucose facilitates A β oligomerization and tau phosphorylation in *C. elegans* model of Alzheimer's disease. *bioRxiv* 228437 doi: <https://doi.org/10.1101/228437>.
- [99] Hetényi C, van der Spoel D. Blind docking of drug-sized compounds to proteins with up to a thousand residues. *FEBS Lett.* 2006;580(5):1447-50.
- [100] Hassan NM, Alhossary AA, Mu Y, Kwok CK. Protein-ligand blind docking using quickVina-W with inter-process spatio-temporal integration. *Sci Rep.* 2017;7(1):15451.
- [101] Ludlow RF, Verdonk ML, Saini HK, Tickle IJ, Jhoti H. Detection of secondary binding sites in proteins using fragment screening. *Proc Natl Acad Sci U S A.* 2015;112:15910-5.
- [102] Orłowski R, Clark JA, Derr JB, Espinoza EM, Mayther MF, Staszewska-Krajewska O, Winkler JR, Jędrzejewska H, Szumna A, Gray HB, Vullev VI, Gryko DT. Role of intramolecular hydrogen bonds in promoting electron flow through amino acid and oligopeptide conjugates. *Proc Natl Acad Sci U S A.* 2021;118:e2026462118.
- [103] Arthur DE, Uzairu A. Molecular docking studies on the interaction of NCI anticancer analogues with human Phosphatidylinositol 4,5-bisphosphate 3-kinase catalytic subunit. *J King Saud Univ Sci.* 2019;31:1151-66.
- [104] Sharath Babu GR, Anand T, Ilaiyaraja N, Khanum F, Gopalan N. Pelargonidin modulates keap1/Nrf2 pathway gene expression and ameliorates citrinin-induced oxidative stress in HepG2 cells. *Front Pharmacol.* 2017;8:868.
- [105] Sohanaki H, Baluchnejadmojarad T, Nikbakht F, Roghani M. Pelargonidin improves memory deficit in amyloid β 25-35 rat model of Alzheimer's disease by inhibition of glial activation, cholinesterase, and oxidative stress. *Biomed Pharmacother.* 2016;83:85-91.
- [106] Mirshekar M, Roghani M, Khalili M, Baluchnejadmojarad T, Arab Moazzen S. Chronic oral pelargonidin alleviates streptozotocin-induced diabetic neuropathic hyperalgesia in rat: Involvement of oxidative stress. *Iran Biomed J.* 2010;14(1-2):33-9.
- [107] Imamura T, Isozumi N, Higashimura Y, Koga H, Segawa T, Desaka N, Takagi H, Matsumoto K, Ohki S, Mori M. Red-beet betalain pigments inhibit amyloid- β aggregation and toxicity in amyloid- β expressing *caenorhabditis elegans*. *Plant Foods Hum Nutr.* 2022;77(1):90-7.

- [108] Meng S, Cao J, Feng Q, Peng J, Hu Y. Roles of chlorogenic Acid on regulating glucose and lipids metabolism: A review. *Evid Based Complement Alternat Med.* 2013;2013:801457.
- [109] Yu CW, Li WH, Hsu FL, Yen PL, Chang ST, Liao VH. Essential oil alloaromadendrene from mixed-type *Cinnamomum osmophloeum* leaves prolongs the lifespan in *Caenorhabditis elegans*. *J Agric Food Chem.* 2014;62(26):6159-65.
- [110] Guo E, Hu Y, Du T, Zhu H, Chen L, Qu W, Zhang J, Xie N, Liu W, Feng F, Xu J. Effects of *Picrasma quassioides* and its active constituents on Alzheimer's disease *in vitro* and *in vivo*. *Bioorg Chem.* 2019;92:103258.
- [111] Agrawal R, Sethiya NK, Mishra SH. Antidiabetic activity of alkaloids of *Aerva lanata* roots on streptozotocin-nicotinamide induced type-II diabetes in rats. *Pharm Biol.* 2013;51(5):635-42.
- [112] Gao X, Wang C, Chen Z, Chen Y, Santhanam RK, Xue Z, Ma Q, Guo Q, Liu W, Zhang M, Chen H. Effects of N-transferuloyltyramine isolated from laba garlic on antioxidant, cytotoxic activities and H₂O₂-induced oxidative damage in HepG2 and L02 cells. *Food Chem Toxicol.* 2019;130:130-41.